Measurement of the *W* boson mass at ATLAS

Arantxa Ruiz Martínez (Carleton),
on behalf of the ATLAS Collaboration

Rencontres de Moriond
QCD and High Energy Interactions

La Thuile, March 25 - April 1, 2017

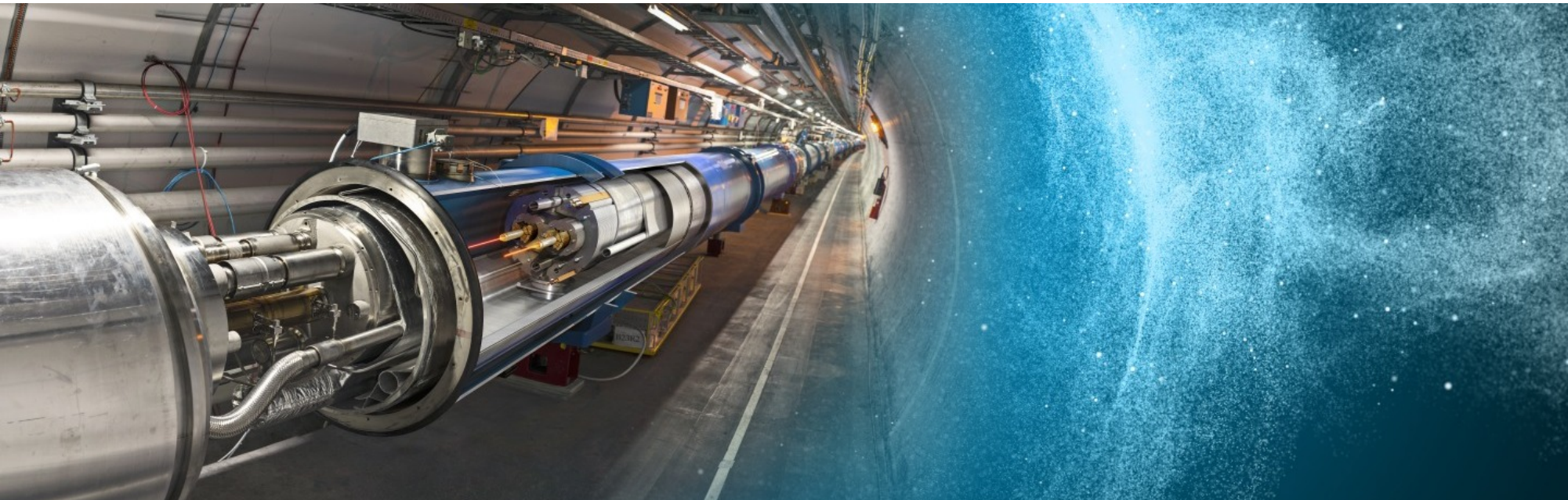

Motivations

- Precision determination of the W mass is a crucial test of the internal consistency of the SM
- W mass can be expressed in terms of the other SM parameters:

$$m_W^2 \left(1 - \frac{m_W^2}{m_Z^2}\right) = \frac{\pi\alpha}{\sqrt{2}G_\mu}(1+\Delta r)$$

- Δr incorporates higher-order corrections, with dependence on m_t and m_H and sensitivity to BSM contributions
- The relation between m_W, m_t and m_H provides a stringent test of the SM and is sensitive to new physics

arXiv:1407.3792

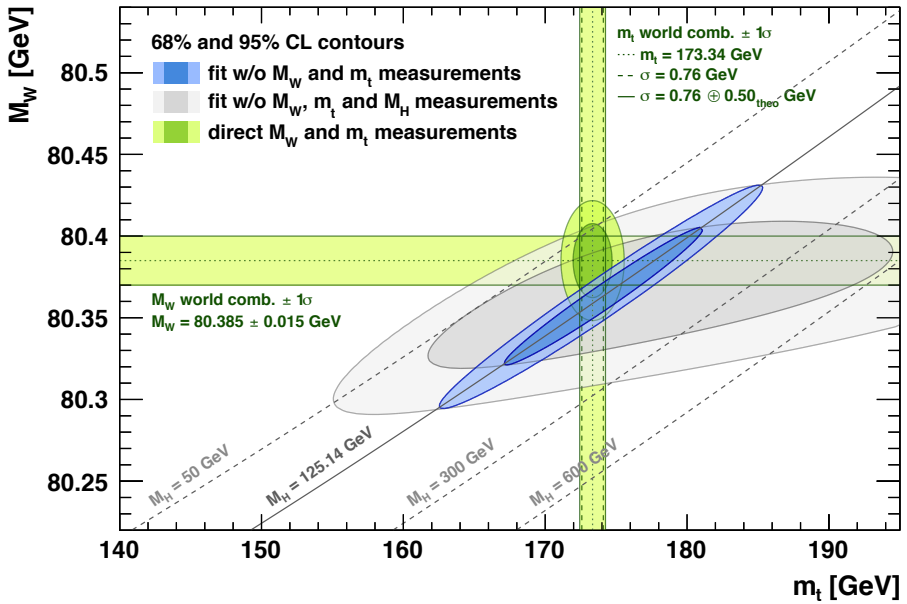

Motivations

- SM predictions (JHEP 12 (2016) 135):
  $m_H = 102.8 \pm 26.3$ GeV
  $m_t = 176.6 \pm 2.5$ GeV
  $m_W = 80.360 \pm 0.008$ GeV
- M_W measurement is the bottleneck, where the experimental uncertainty is worse than the theoretical one

Phys. Rev. D 88 (2013) 052018

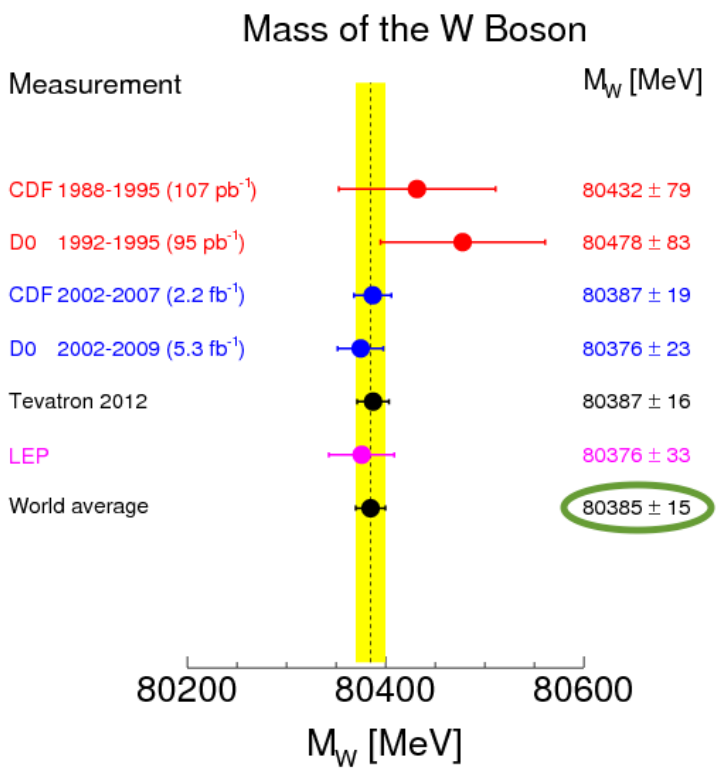

Phys. Rev. Lett. 114 (2015) 191803

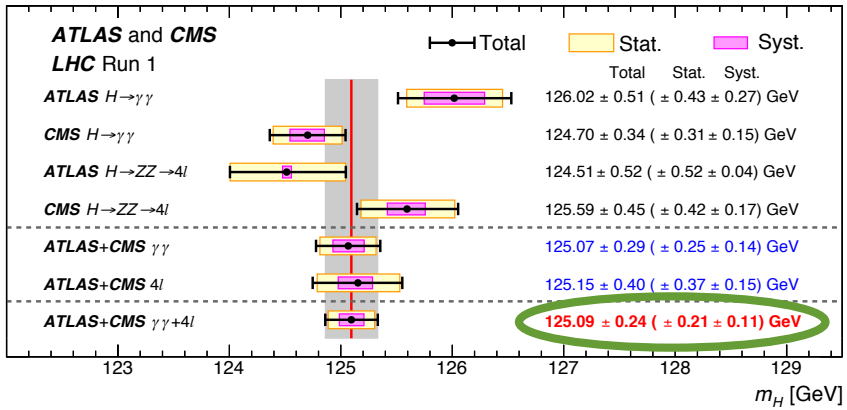

LHCTopWGSummaryPlots

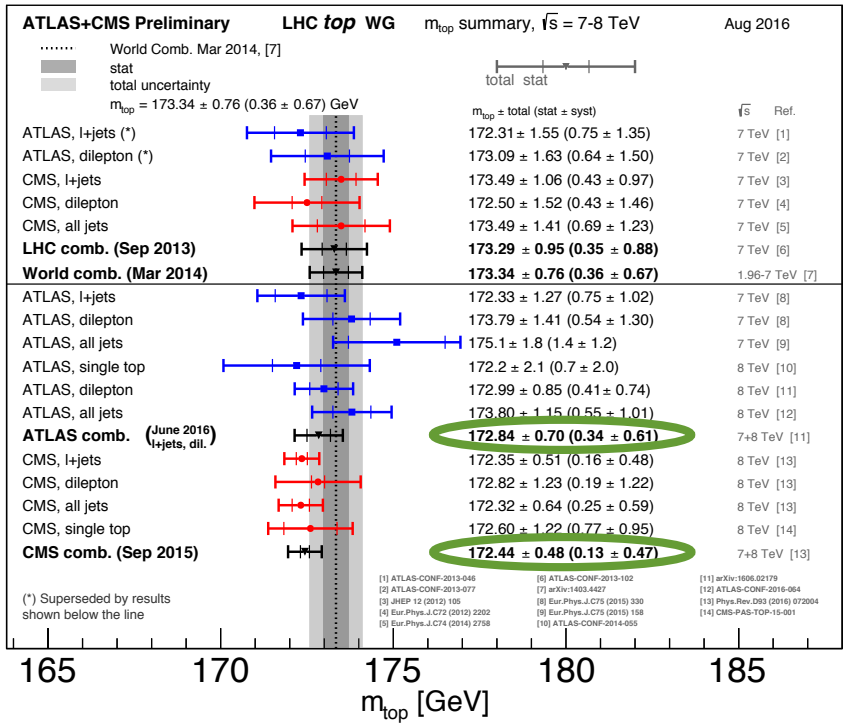

LHC versus Tevatron

- Tevatron: W^+/W^- production is symmetric, dominated by interactions with at least one valence quark
- W^+/W^- production at the LHC is asymmetric $\rightarrow$ Charge-dependent analysis
- The sea-quark PDFs play a larger role at the LHC
- W-mass measurement sensitive to s and c PDFs (implications in the W p_{T} distributions): 25% of the W-boson production is induced by at least one second generation quark at the LHC, only 5% at Tevatron
- Very challenging to achieve at the LHC an experimental precision similar to Tevatron

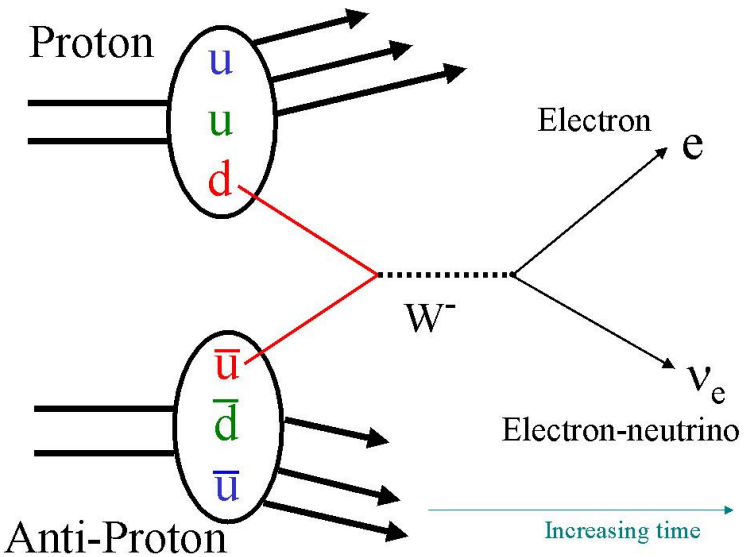

Measurement overview

$\Rightarrow$ 2011 ATLAS data at $\sqrt{s} = 7$ TeV, 4.6 fb^{-1} (e channel), 4.1 fb^{-1} (μ channel)

$\Rightarrow$ Moderate average number of interactions per bunch crossing $\langle\mu\rangle = 9.1$

Event selection

Selection requirements optimised to reduce the background where we cannot assure to have a good calibration

- Exactly one electron ($|\eta| < 1.2$ or $1.8 < |\eta| < 2.4$) or muon ($|\eta| < 2.4$), p_{T}^{ℓ}>30 GeV
- Recoil $u_{\mathrm{T}} < 30$ GeV (minimise model uncertainties from W produced at high p_{T})
  - Vector sum of the E_{T} of all calorimeter clusters: $\overrightarrow{u}_{\mathrm{T}} = \sum_i \overrightarrow{E}_{\mathrm{T},i}$
  - In W and Z events, $-\overrightarrow{u}_{\mathrm{T}}$ provides a measure of the boson p_{T}
- Missing transverse momentum $p_{\mathrm{T}}^{\mathrm{miss}} > 30$ GeV
- Transverse mass $m_{\mathrm{T}} = \sqrt{2 p_{\mathrm{T}}^{\ell} p_{\mathrm{T}}^{\mathrm{miss}} (1 - \cos\Delta\phi)} > 60$ GeV
- Selected sample: 5.9×10^6 $W \to e\nu$ and 7.8×10^6 $W \to \mu\nu$ events

Calibration sample

- Z events used to calibrate the response of the detector to electrons and muons, and to derive recoil corrections
- Exactly two leptons with $p_{\mathrm{T}}^{\ell} > 25$ GeV, same flavour and opposite charges
- $80 < m_{\ell\ell} < 100$ GeV
- Calibration sample: 0.6×10^6 $Z \to ee$ and 1.2×10^6 $Z \to \mu\mu$ events

Measurement overview

Analysis strategy

- Template fits to sensitive distributions: p_{T}^{ℓ}, m_{T} and $p_{\mathrm{T}}^{\mathrm{miss}}$ (used as cross-check)

p_{T}^{ℓ} has a Jacobian edge at $m_W/2$

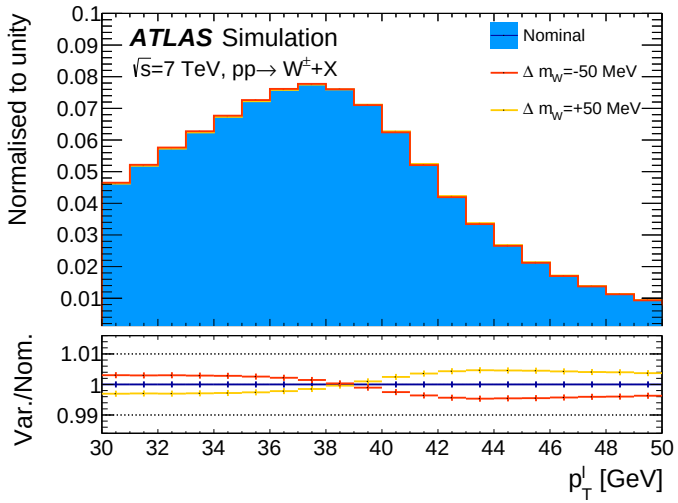

m_{T} has an endpoint at m_W

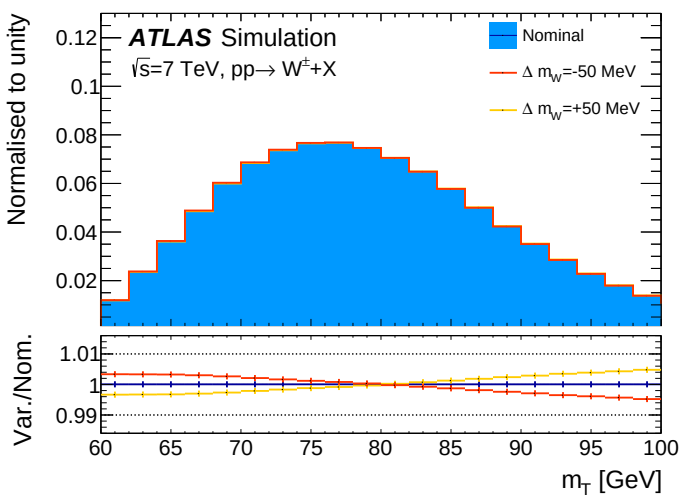

- Templates simulated for several values of m_W and compared to the observed distribution by means of χ^2 test (templates include signal and background)
- The χ^2 function is interpolated a second order polynomial and the minimum of the χ^2 function yields the extracted value of m_W
- Final result obtained combining the individual m_W measurements in several categories (categories defined to reduce the uncertainties)

Decay channel	$W \to e\nu$	$W \to \mu\nu$
Kinematic distributions	p_{T}^{ℓ}, m_{T}	p_{T}^{ℓ}, m_{T}
Charge categories	W^+, W^-	W^+, W^-
$\lvert\eta_\ell\rvert$ categories	$[0, 0.6]$, $[0.6, 1.2]$, $[1.8, 2.4]$	$[0, 0.8]$, $[0.8, 1.4]$, $[1.4, 2.0]$, $[2.0, 2.4]$

Muon calibration

⇒ Corrections for momentum scale and resolution, and for reconstruction, isolation, and trigger efficiencies are applied to the muons in the simulated events

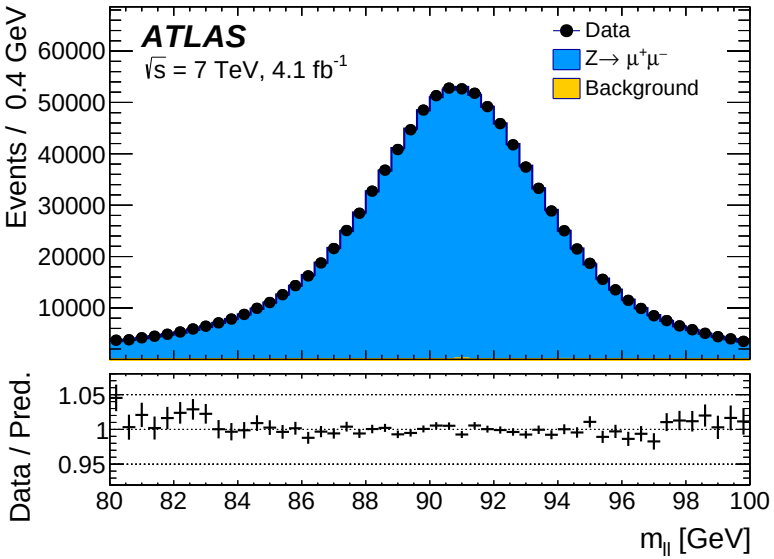

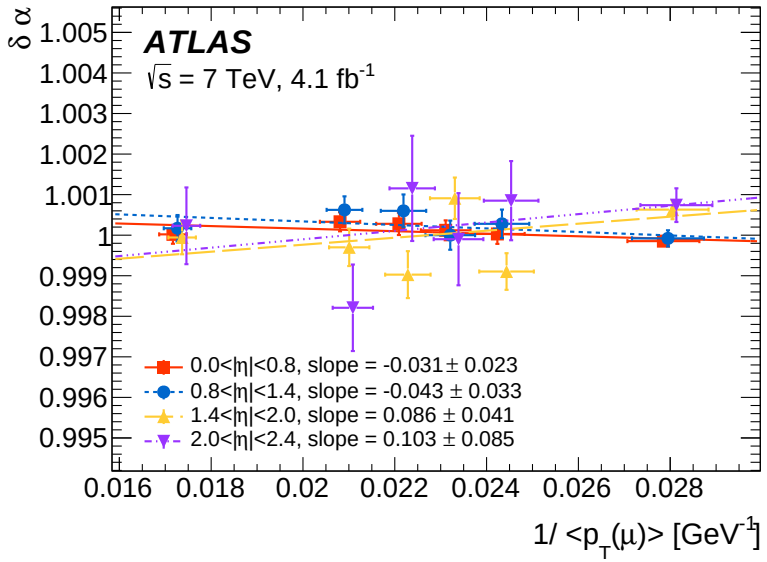

⇒ Systematic uncertainties in the m_W measurement due to muon calibration and efficiency corrections averaged over lepton charge

$\lvert\eta_\ell\rvert$ range	$[0.0, 0.8]$		$[0.8, 1.4]$		$[1.4, 2.0]$		$[2.0, 2.4]$		Combined	
Kinematic distribution	p_{T}^{ℓ}	m_{T}	p_{T}^{ℓ}	m_{T}	p_{T}^{ℓ}	m_{T}	p_{T}^{ℓ}	m_{T}	p_{T}^{ℓ}	m_{T}
δm_W [MeV]										
Momentum scale	8.9	9.3	14.2	15.6	27.4	29.2	111.0	115.4	8.4	8.8
Momentum resolution	1.8	2.0	1.9	1.7	1.5	2.2	3.4	3.8	1.0	1.2
Sagitta bias	0.7	0.8	1.7	1.7	3.1	3.1	4.5	4.3	0.6	0.6
Reconstruction and isolation efficiencies	4.0	3.6	5.1	3.7	4.7	3.5	6.4	5.5	2.7	2.2
Trigger efficiency	5.6	5.0	7.1	5.0	11.8	9.1	12.1	9.9	4.1	3.2
Total	11.4	11.4	16.9	17.0	30.4	31.0	112.0	116.1	9.8	9.7

Calibration of the recoil

⇒ Recoil projections:

- $u_{\parallel}^{Z}$: parallel projection on the Z direction (scale)
- $u_{\perp}^{Z}$: perpendicular projection on the Z direction (resolution)
- $u_{\parallel}^{\ell}$: parallel projection on the lepton direction (W events)

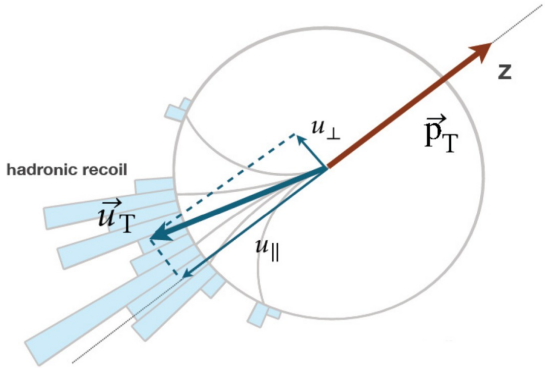

⇒ Recoil calibration procedure performed in two steps:

- u_T resolution mismodelling addressed with event activity corrections, such as pileup, residual differences in the $\sum E_T$ distributions (derived separately for W and Z events)
- Residual corrections using p_T balance between lepton pairs and recoil in Z events

⇒ Systematic uncertainties in the m_W measurement due to recoil corrections

W-boson charge	W^+		W^-		Combined	
Kinematic distribution	p_T^ℓ	m_T	p_T^ℓ	m_T	p_T^ℓ	m_T
δm_W [MeV]						
$\langle\mu\rangle$ scale factor	0.2	1.0	0.2	1.0	0.2	1.0
$\Sigma\bar{E}_T$ correction	0.9	12.2	1.1	10.2	1.0	11.2
Residual corrections (statistics)	2.0	2.7	2.0	2.7	2.0	2.7
Residual corrections (interpolation)	1.4	3.1	1.4	3.1	1.4	3.1
Residual corrections ($Z \to W$ extrapolation)	0.2	5.8	0.2	4.3	0.2	5.1
Total	2.6	14.2	2.7	11.8	2.6	13.0

⇒ Larger uncertainties for the m_W extracted from m_T since p_T^{miss} enters in its definition

Consistency tests with Z-boson events

$\Rightarrow$ Results from the p_{T}^{ℓ} and m_{T} distributions consistent with the LEP combined value of m_Z (91187.5 MeV) within experimental uncertainties

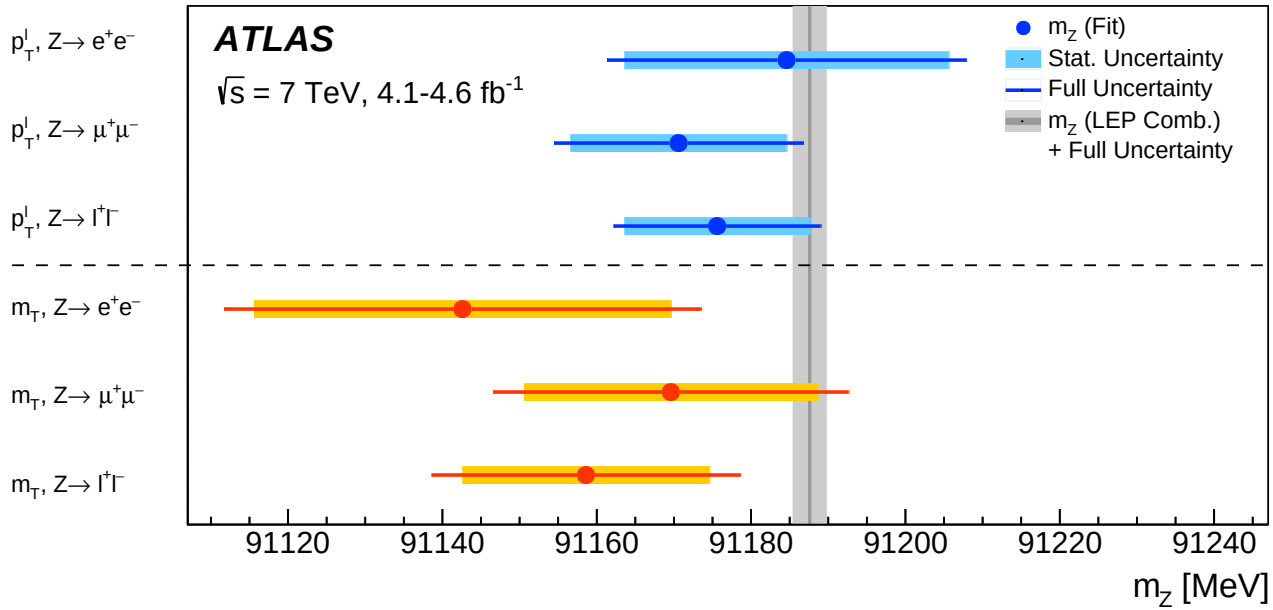

$\Rightarrow$ Difference between the extracted m_Z and the LEP combined value together with the statistical and experimental systematic uncertainties

Lepton charge	ℓ^+		ℓ^-		Combined	
Distribution	p_{T}^{ℓ}	m_{T}	p_{T}^{ℓ}	m_{T}	p_{T}^{ℓ}	m_{T}
Δm_Z [MeV]						
$Z \to ee$	$13 \pm 31 \pm 10$	$-93 \pm 38 \pm 15$	$-20 \pm 31 \pm 10$	$4 \pm 38 \pm 15$	$-3 \pm 21 \pm 10$	$-45 \pm 27 \pm 15$
$Z \to \mu\mu$	$1 \pm 22 \pm 8$	$-35 \pm 28 \pm 13$	$-36 \pm 22 \pm 8$	$-1 \pm 27 \pm 13$	$-17 \pm 14 \pm 8$	$-18 \pm 19 \pm 13$
Combined	$5 \pm 18 \pm 6$	$-58 \pm 23 \pm 12$	$-31 \pm 18 \pm 6$	$1 \pm 22 \pm 12$	$-12 \pm 12 \pm 6$	$-29 \pm 16 \pm 12$

$\Rightarrow$ This is not a measurement of m_Z since it is used as input for the calibration

Background estimation

Background contributions estimated using simulation:

- $Z \to \ell\ell$ is the dominant background
  - $Z \to ee$ is up to 4.0% in the electron channel
  - $Z \to \mu\mu$ is up to 6.3% in the muon channel
- $Z \to \tau\tau$ (0.12%), $W \to \tau\nu$ (1.0%), top-quark (0.11%), dibosons (0.07%)

Multijet background contribution estimated using data-driven techniques:

- Relies on template fits to kinematic distributions ($p_{\mathrm{T}}^{\mathrm{miss}}$, m_{T} and $p_{\mathrm{T}}^{\ell}/m_{\mathrm{T}}$) in background-dominated regions (FR1 and FR2)
- Template fits are done in slices of isolation and then the final multijet fraction is extrapolated to the SR isolation

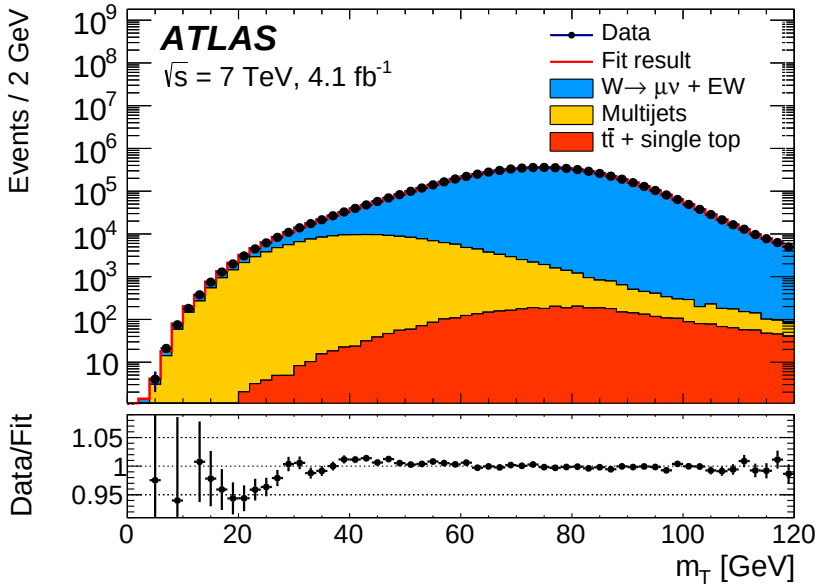

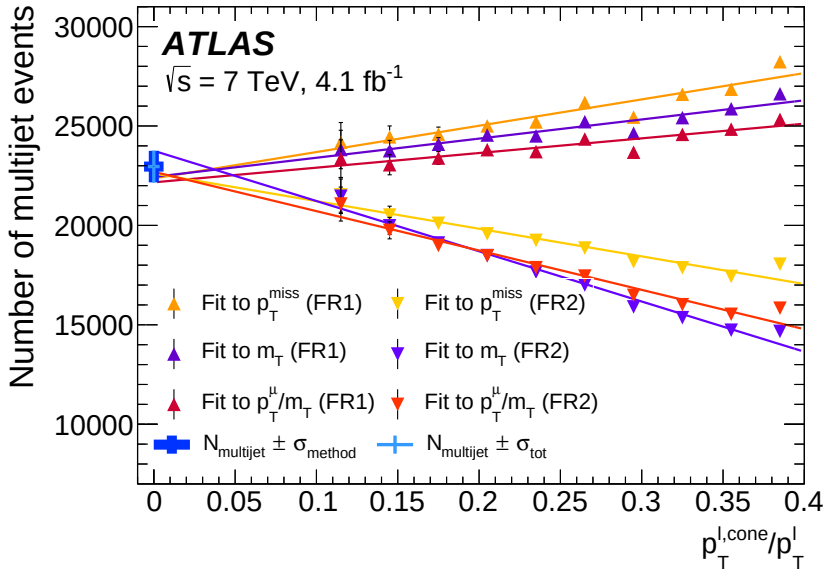

Physics modelling

W POWHEG+PYTHIA 8 samples are reweighted to include the effects of higher-order QCD and EW corrections, and fits to measured distributions to improve agreement with data

EWK effects:

- QED FSR and ISR included in the MC
- Uncertainties for non-included effects: interference between ISR and FSR, virtual-loop and box diagrams, and FSR lepton pair production

QCD corrections:

- Reweighting of the rapidity and angular variables to NNLO, and p_{T}^{W} to PYTHIA 8 AZ tune

Rapidity distributions and angular coefficients:

- Modelled with fixed-order perturbative QCD with DYNNLO and CT10nnlo PDF
- Validated in $Z \to \ell\ell$, uncertainties for angular disagreements with data

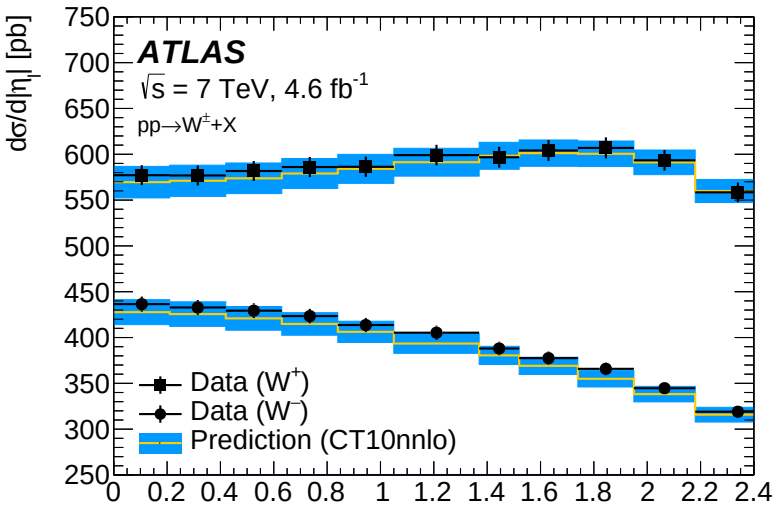

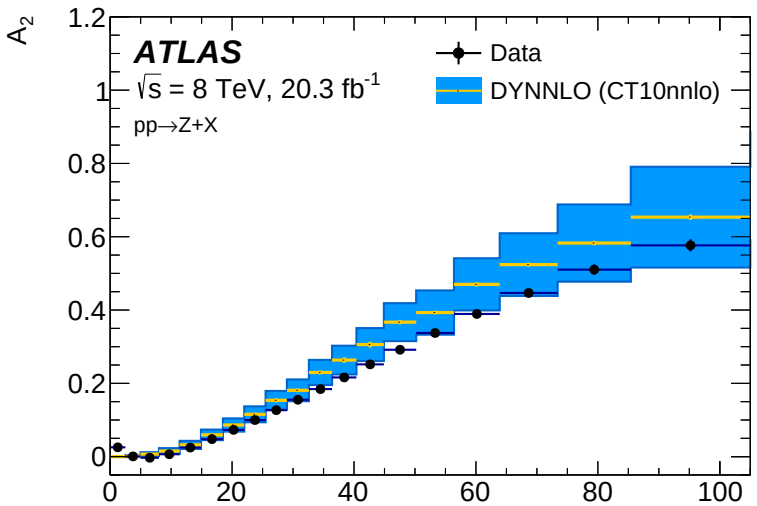

p_{T}^{W} distribution

The $u_{\parallel}^{\ell}$ distribution is very sensitive to the underlying p_{T}^{W} distribution:

$\Rightarrow$ PYTHIA 8 AZ used (tuned to the ATLAS p_{T}^{Z} measurement)

$\Rightarrow$ DYRES prediction clearly disfavored by data

$\Rightarrow$ Powheg MiNLO+Pythia 8 predict a harder p_{T}^{W} spectrum

JHEP 09 (2014) 145

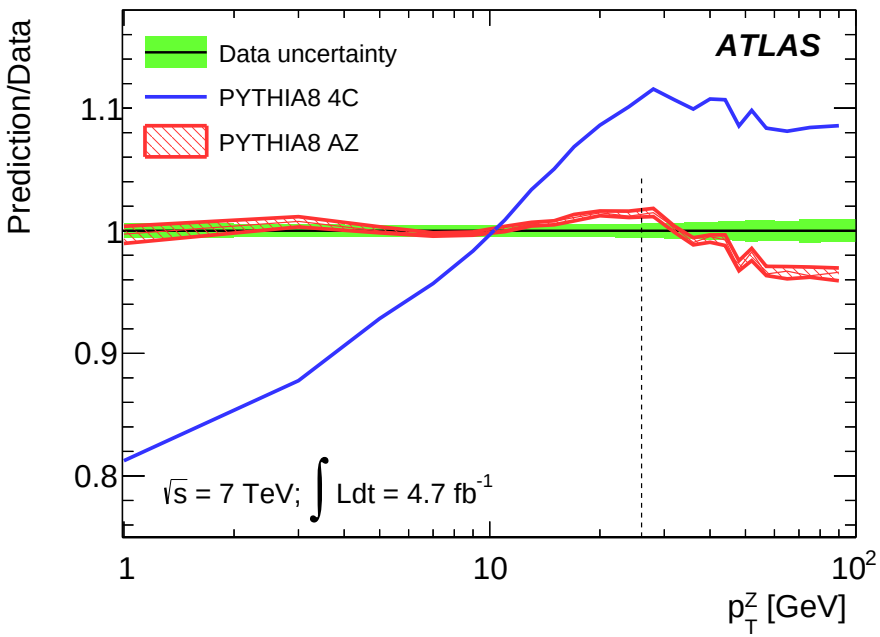

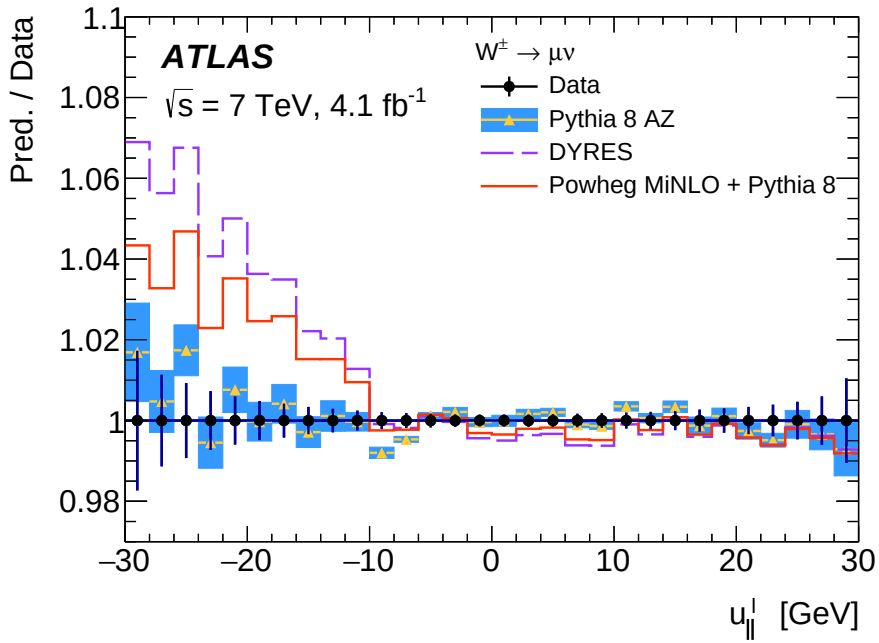

Physics modelling uncertainties

- Fixed-order PDF uncertainty (dominant):
  - CT10nnlo PDF variations
  - Envelope from MMHT2014 and CT14 NNLO PDFs
- PYTHIA 8 PS AZ tune parameter uncertainties
- Charm-quark mass uncertainty ($m_c \pm 0.5$ GeV)
- Parton shower scale uncertainties
- Parton shower PDF uncertainty:
  - PYTHIA 8 PS employs CTEQ6L1 LO PDF
  - Envelope from CT14lo, MMHT2014lo and NNPDF2.3lo
- Angular coefficients:
  - A_i uncertainties from Z data (JHEP 08 (2016) 159)

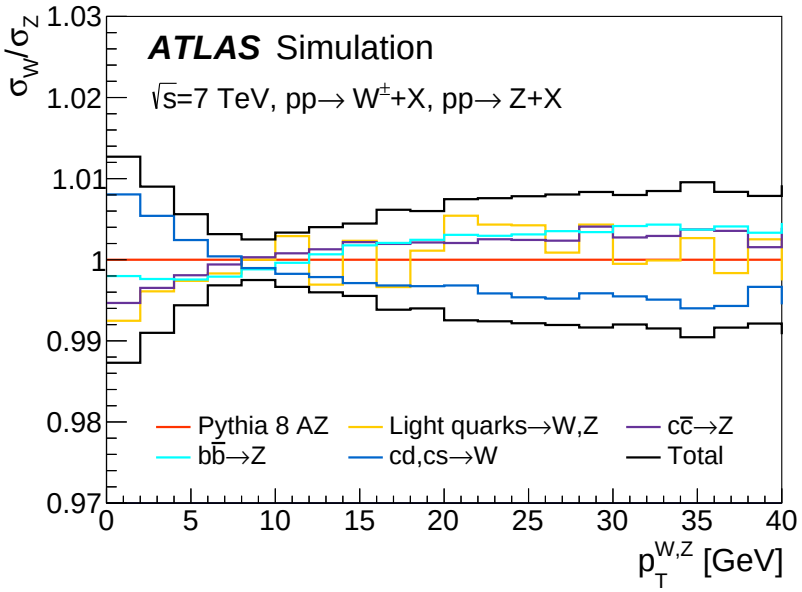

W-boson charge	W^+		W^-		Combined	
Kinematic distribution	p_{T}^{ℓ}	m_{T}	p_{T}^{ℓ}	m_{T}	p_{T}^{ℓ}	m_{T}
δm_W [MeV]						
Fixed-order PDF uncertainty	13.1	14.9	12.0	14.2	8.0	8.7
AZ tune	3.0	3.4	3.0	3.4	3.0	3.4
Charm-quark mass	1.2	1.5	1.2	1.5	1.2	1.5
Parton shower μ_{F} with heavy-flavour decorrelation	5.0	6.9	5.0	6.9	5.0	6.9
Parton shower PDF uncertainty	3.6	4.0	2.6	2.4	1.0	1.6
Angular coefficients	5.8	5.3	5.8	5.3	5.8	5.3
Total	15.9	18.1	14.8	17.2	11.6	12.9

Mass-sensitive distributions

η-inclusive p_{T}^{ℓ} and m_{T} distributions

Closure test:

$\Rightarrow$ Data compared to the simulation including signal and background contributions

$\Rightarrow$ Detector calibration and physics-modelling corrections applied to the simulation

$\Rightarrow$ m_W used in the predictions set to the overall measurement result

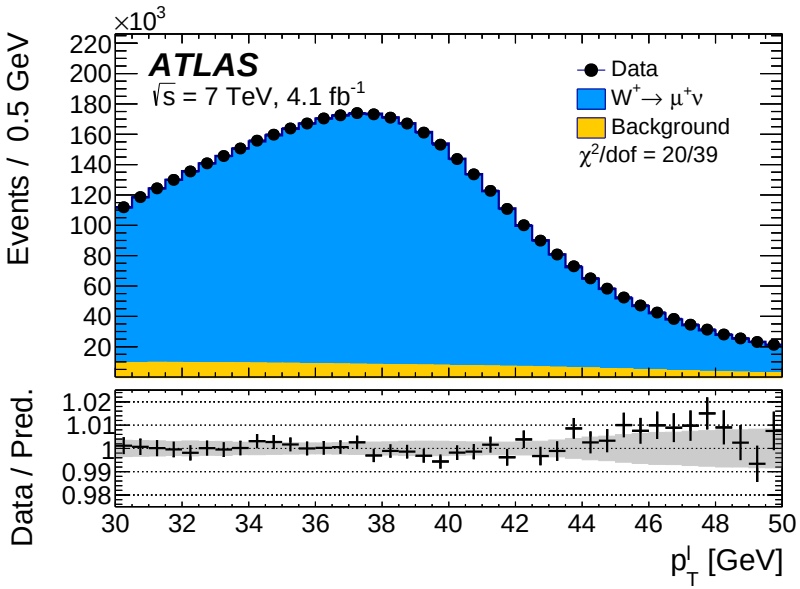

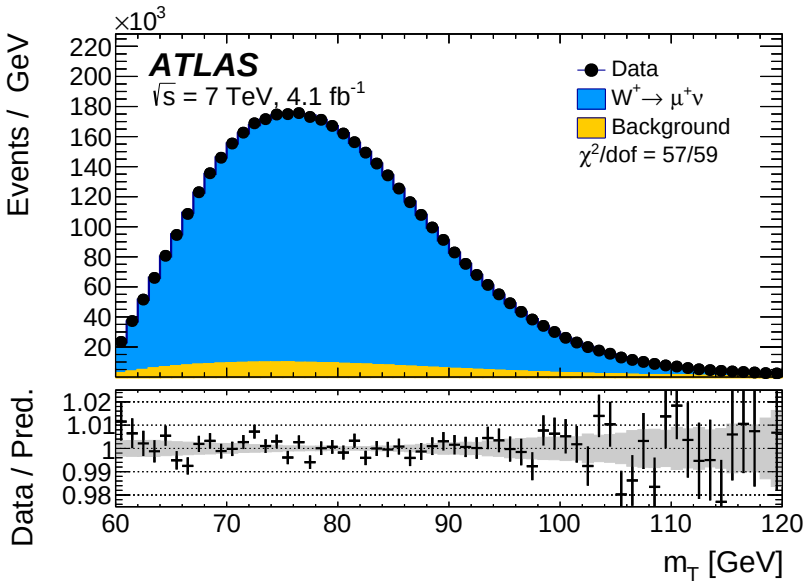

Results in the different categories

- A total of 28 m_W determinations $\Rightarrow$ Compatibility of categories constitutes a strong validation of the calibration and physics modelling
- Fitting ranges optimized to lead to the smallest uncertainties on Monte Carlo ($32 < p_{\mathrm{T}}^{\ell} < 45$ GeV and $66 < m_{\mathrm{T}} < 99$ GeV)

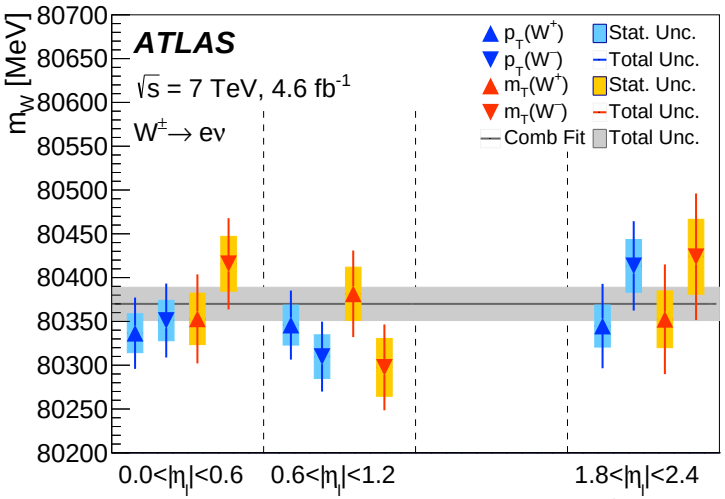

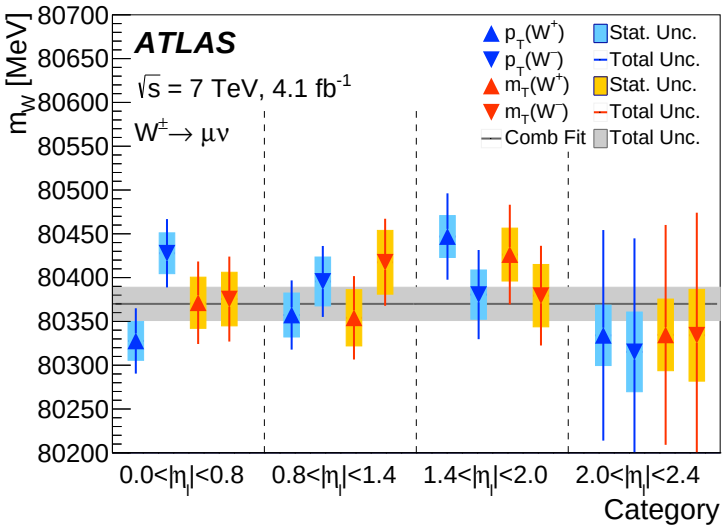

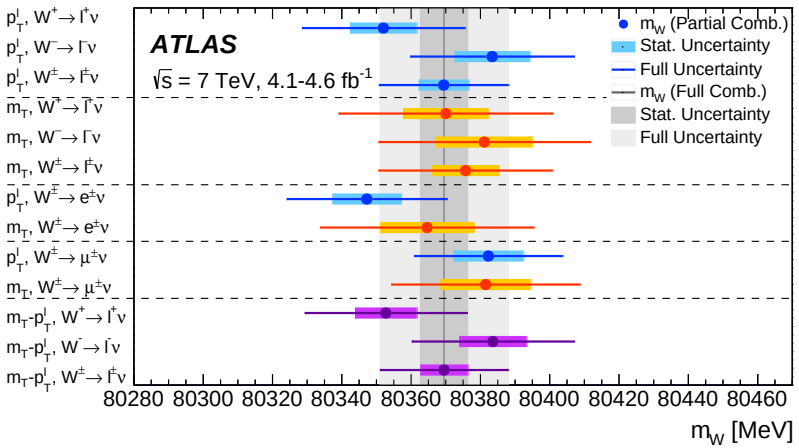

Final results

Overview of the different m_W measurements

$m_W = 80370 \pm 7$ (stat.) ± 11 (exp. syst.) ± 14 (mod. syst.) MeV $= 80370 \pm 19$ MeV

$\Rightarrow$ Competitive to the most precise single measurements by the Tevatron experiments:

- $m_W = 80387 \pm 19$ MeV by CDF (Phys. Rev. Lett. 108 (2012) 151803)
- $m_W = 80375 \pm 23$ MeV by DØ (Phys. Rev. Lett. 108 (2012) 151804)

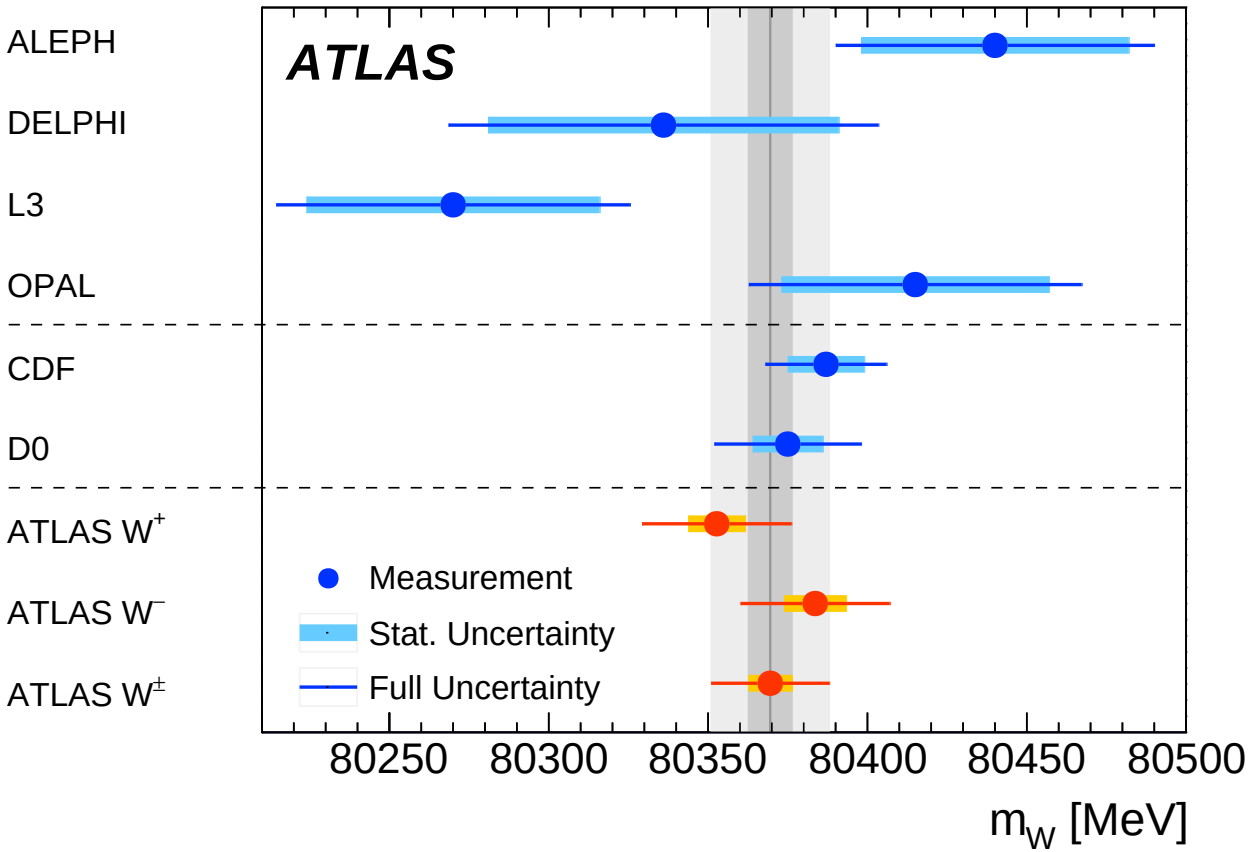

Final results

$m_W = 80370 \pm 7$ (stat.) ± 11 (exp. syst.) ± 14 (mod. syst.) MeV $= 80370 \pm 19$ MeV

$\Rightarrow$ Result consistent with the SM expectation ($m_W = 80358 \pm 8$ MeV) and compatible with the PDG world average ($m_W = 80385 \pm 15$ MeV)

$\Rightarrow$ Result sits in between the Tevatron measurement and the SM prediction reducing the tension and shrinking the space for new physics

SM prediction of m_W from the global electroweak fit using:
$m_t = 172.84 \pm 0.70$ GeV
$m_H = 125.09 \pm 0.24$ GeV

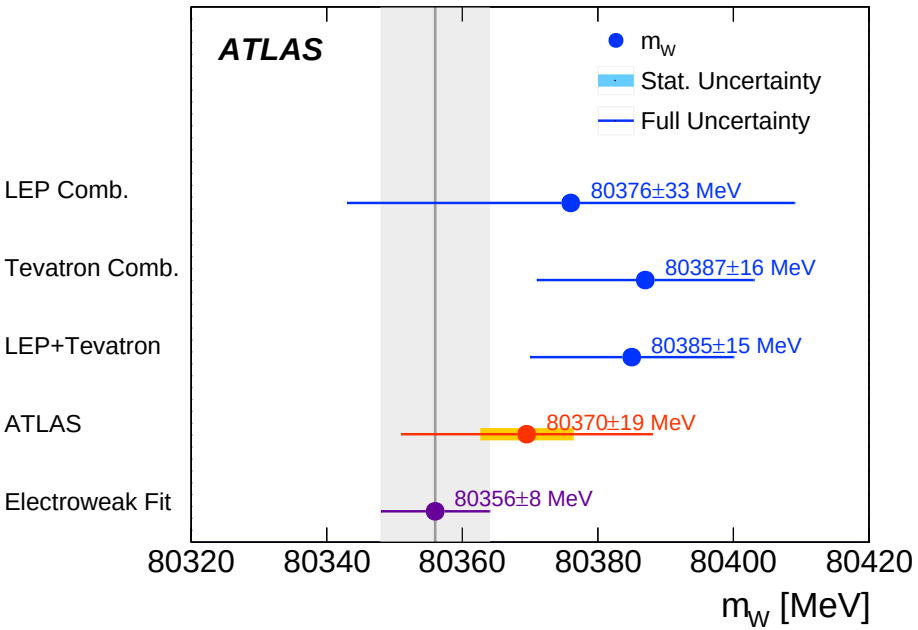

Indirect determination of m_W and m_t from the global electroweak fit assuming $m_H = 125.09 \pm 0.24$ GeV compared to the ATLAS measurements

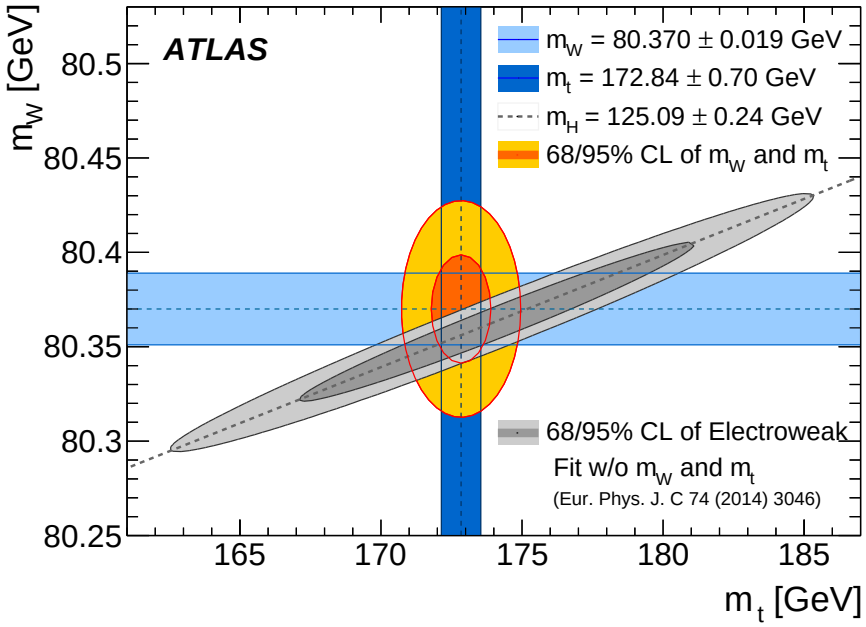

Conclusions

- Huge milestone of the LHC program!
- W-boson mass measured using 2011 data at $\sqrt{s} = 7$ TeV corresponding to 4.6 fb^{-1} by ATLAS (arXiv:1701.07240):

$$\begin{aligned} m_W &= 80370 \pm 7\ (\text{stat.}) \pm 11\ (\text{exp. syst.}) \pm 14\ (\text{mod. syst.})\ \text{MeV} \\ &= 80370 \pm 19\ \text{MeV} \end{aligned}$$

- Measurement determined from template fits in the p_{T}^{ℓ} and m_{T} distributions, for W^+ and W^-, in the electron and muon channels, and in several kinematic categories
- Consistent with the SM expectation ($m_W = 80358 \pm 8$ MeV) and compatible with the current world average ($m_W = 80385 \pm 15$ MeV)
- ATLAS measurement comparable in precision to the currently leading measurements by CDF and DØ
- The modelling uncertainties currently dominate the overall uncertainty of the m_W measurement

BACKUP

Overview of the different m_W measurements

CDF experiment (Phys. Rev. Lett. 108 (2012) 151803):

- Electron and muon channels
- 2.2 fb^{-1} integrated luminosity
- $m_W = 80387 \pm 19$ MeV

DØ experiment (Phys. Rev. Lett. 108 (2012) 151804):

- Electron channel
- 5.3 fb^{-1} integrated luminosity
- $m_W = 80375 \pm 23$ MeV

ATLAS experiment (arXiv:1701.07240):

- Electron and muon channels
- 4.6 fb^{-1} integrated luminosity
- $m_W = 80370 \pm 19$ MeV

Muon calibration

Muon momentum calibration

- Momentum scale and resolution corrections derived using $Z \to \mu\mu$ decays

$$p_{\mathrm{T}}^{\mathrm{MC,corr}} = p_{\mathrm{T}}^{\mathrm{MC}} \times [1+\alpha(\eta,\phi)] \times \left[1+\beta_{\mathrm{curv}}(\eta)\cdot G(0,1)\cdot p_{\mathrm{T}}^{\mathrm{MC}}\right],$$

$$p_{\mathrm{T}}^{\mathrm{data,corr}} = \frac{p_{\mathrm{T}}^{\mathrm{data}}}{1+q\cdot\delta(\eta,\phi)\cdot p_{\mathrm{T}}^{\mathrm{data}}},$$

- Two methods are used for the determination of the sagitta bias
  - $Z \to \mu\mu$ method
  - E/p method

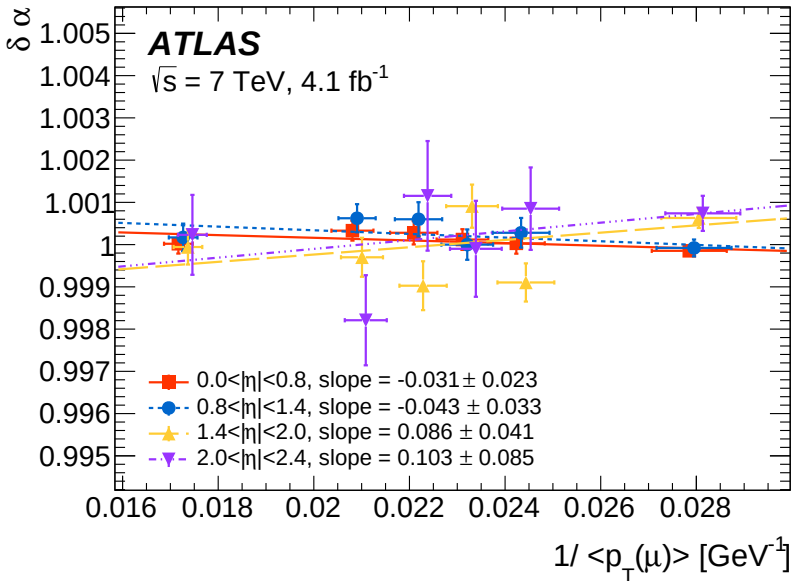

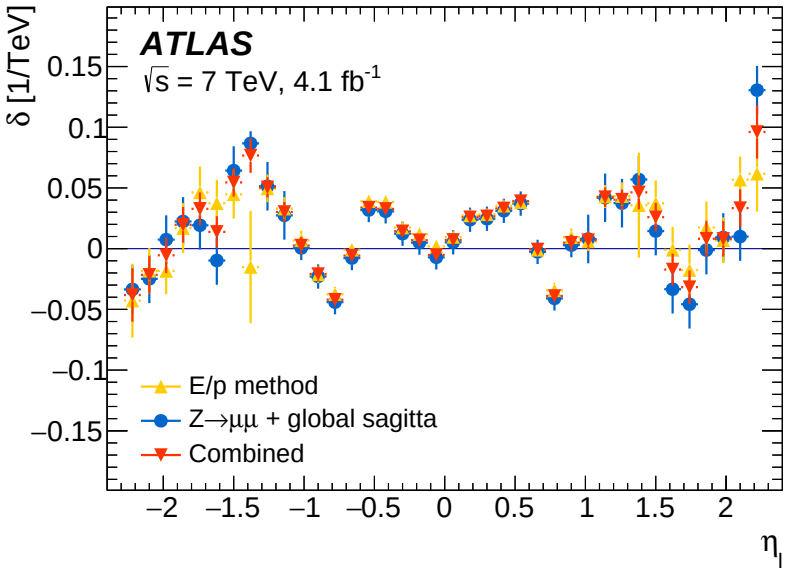

Muon calibration

Muon selection efficiency

- Corrections to the muon reconstruction, trigger and isolation efficiencies estimated using $Z \to \mu\mu$ tag-and-probe in data and simulation
- Corrections evaluated as functions of p_{T}^{ℓ} and $u_{\parallel}^{\ell}$ and in various regions of the detector
- Dependence of the efficiencies on $u_{\parallel}^{\ell}$ agree in data and simulation $\to$ corrections evaluated only as a function of p_{T}^{ℓ} and η_{ℓ}, separately for positive and negative muon charges
- Dominant uncertainty: statistical uncertainty of the Z data sample
- Largest systematics: multijet background contribution and momentum-scale uncertainty
- The corresponding uncertainty in the measurement of m_W is approximately 5 MeV

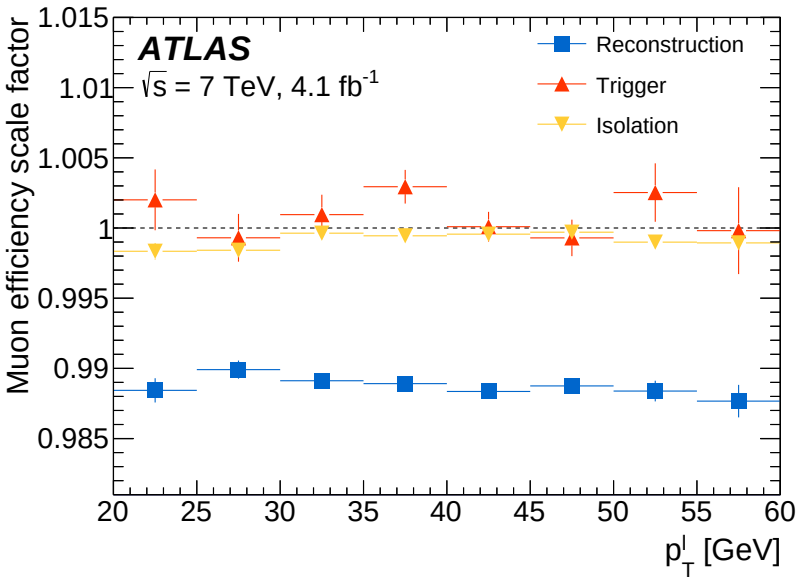

Electron calibration

Corrections for energy resolution, and for reconstruction, identification, isolation and trigger efficiencies are applied to the simulation and energy-scale corrections are applied to the data

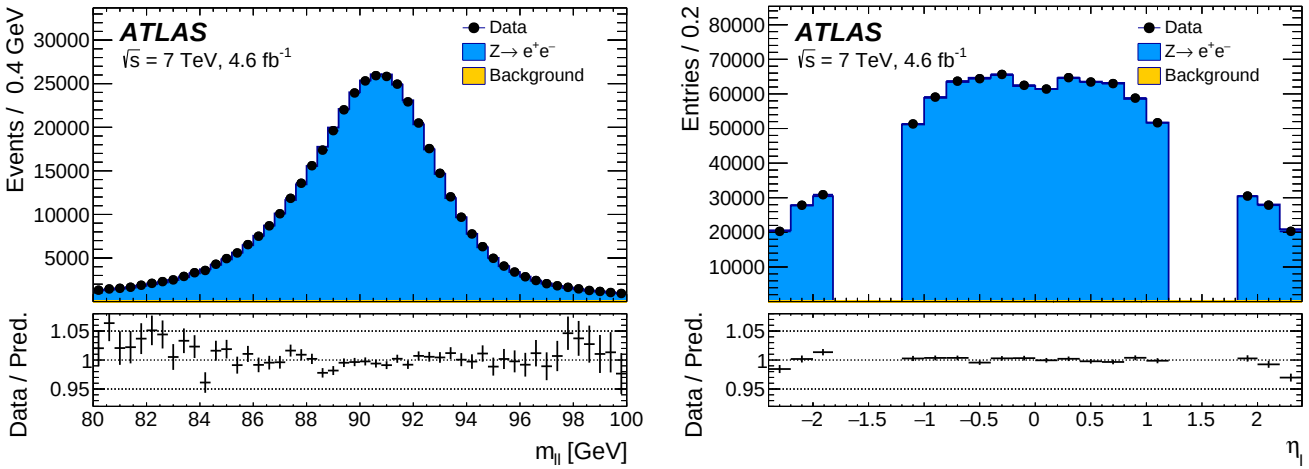

Systematics due to electron energy calibration, efficiency corrections and charge mismeasurement

$\lvert\eta_\ell\rvert$ range	$[0.0, 0.6]$		$[0.6, 1.2]$		$[1.82, 2.4]$		Combined	
Kinematic distribution	p_{T}^{ℓ}	m_{T}	p_{T}^{ℓ}	m_{T}	p_{T}^{ℓ}	m_{T}	p_{T}^{ℓ}	m_{T}
δm_W [MeV]								
Energy scale	10.4	10.3	10.8	10.1	16.1	17.1	8.1	8.0
Energy resolution	5.0	6.0	7.3	6.7	10.4	15.5	3.5	5.5
Energy linearity	2.2	4.2	5.8	8.9	8.6	10.6	3.4	5.5
Energy tails	2.3	3.3	2.3	3.3	2.3	3.3	2.3	3.3
Reconstruction efficiency	10.5	8.8	9.9	7.8	14.5	11.0	7.2	6.0
Identification efficiency	10.4	7.7	11.7	8.8	16.7	12.1	7.3	5.6
Trigger and isolation efficiencies	0.2	0.5	0.3	0.5	2.0	2.2	0.8	0.9
Charge mismeasurement	0.2	0.2	0.2	0.2	1.5	1.5	0.1	0.1
Total	19.0	17.5	21.1	19.4	30.7	30.5	14.2	14.3

Electron calibration

Electron energy response

- Overall energy-scale correction determined as a function of η_ℓ from $Z \to ee$ decays comparing the reconstructed mass distributions in data and simulation

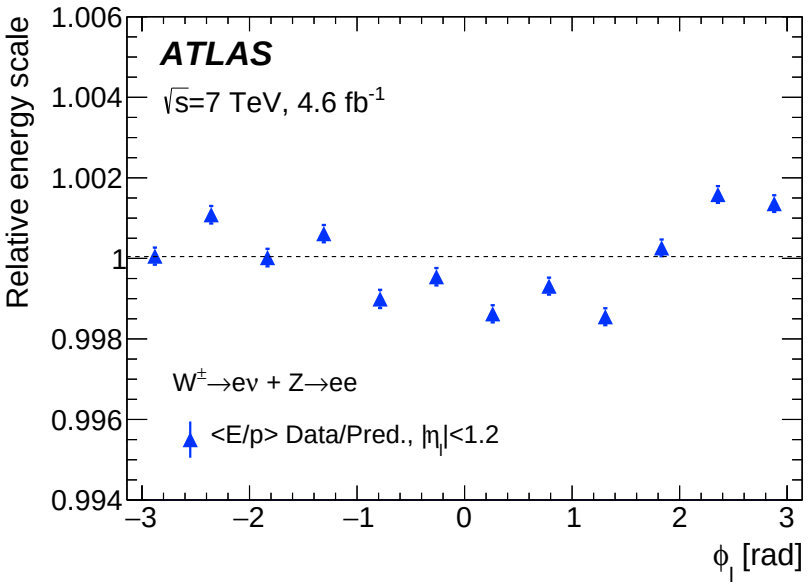

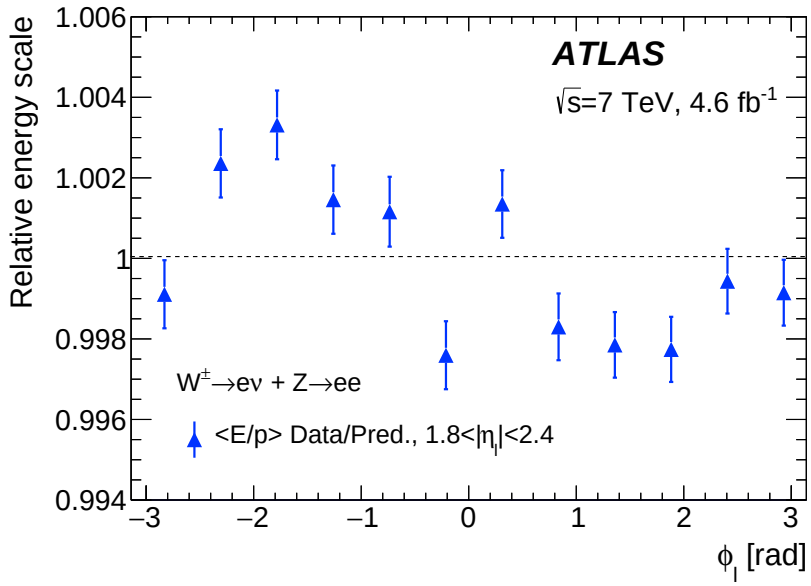

Electron calibration

Electron selection efficiency

- Electron efficiency corrections are determined using samples of $W \to e\nu$, $Z \to ee$ and $J/\psi \to ee$
- Electron reconstruction, identification and trigger efficiencies measured separately as a function of electron η and p_{T}
- Reconstruction and identification efficiency corrections have a typical uncertainty of 0.1-0.2% in the barrel and 0.3% in the endcap
- Trigger efficiency corrections have an uncertainty smaller than 0.1%
- Energy-isolation efficiency corrections deviate from unity by less than 0.5%, with an uncertainty smaller than 0.2% on average
- The rate of electron charge mismeasurement in simulated events rises from about 0.2% in the barrel to 4% in the endcap (agreement with data better than 0.1%)

Calibration of the recoil

Recoil projections:

- $u_{\parallel}$: parallel projection on the boson direction
- $u_{\perp}$: perpendicular projection on the boson direction
- $u_{\parallel}^{\ell}$: parallel projection on the lepton decay (W) direction

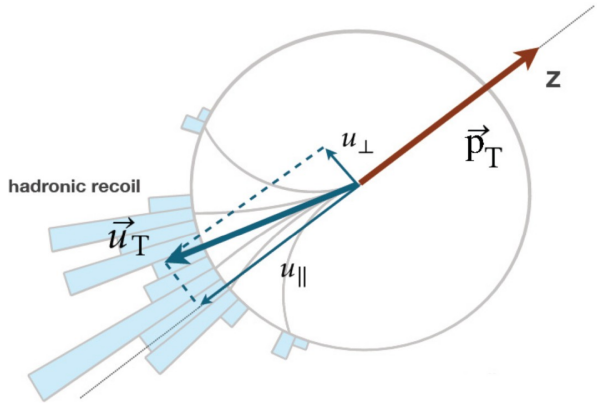

Recoil calibration procedure performed in two steps:

- u_T resolution mismodelling addressed with event activity corrections, such as pileup, residual differences in the $\sum \bar{E}_T$ distributions (derived separately for W and Z events)
- Residual corrections using p_T balance between lepton pairs and recoil in Z events

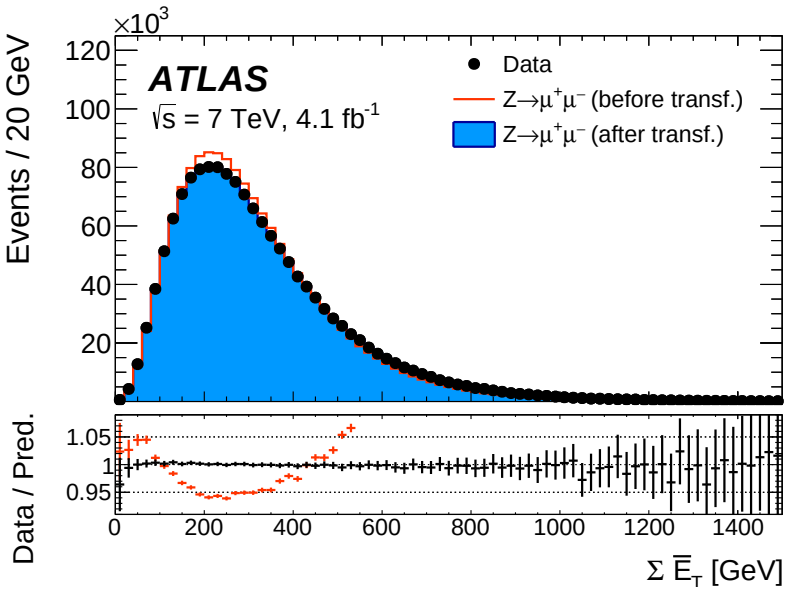

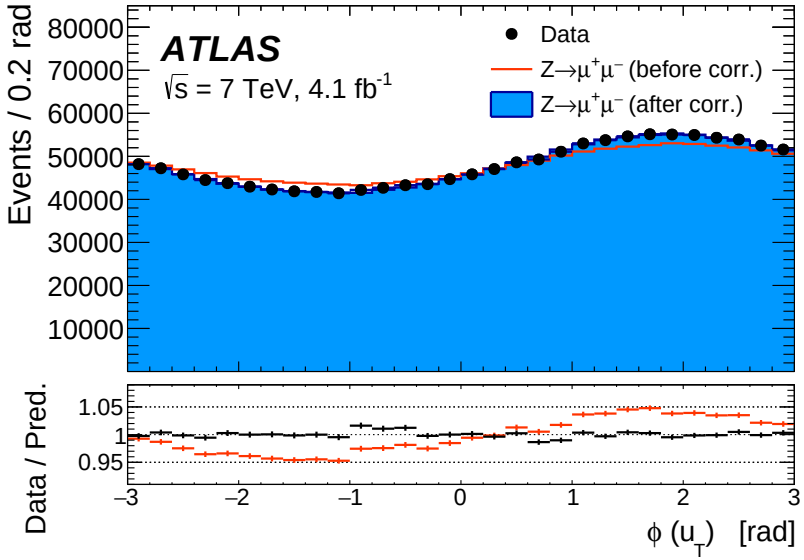

Calibration of the recoil

Recoil distributions in data and simulation before and after applying the recoil corrections

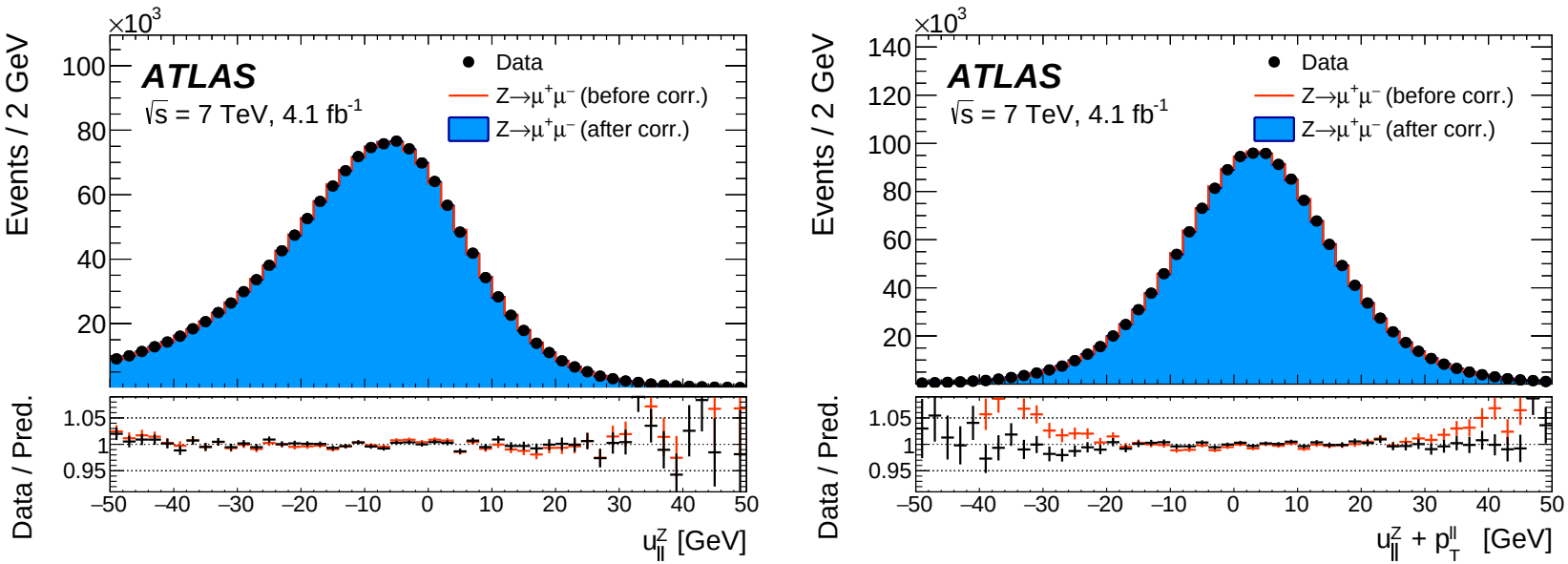

⇒ Systematic uncertainties in the m_W measurement due to recoil corrections

W-boson charge	W^+		W^-		Combined	
Kinematic distribution	p_{T}^{ℓ}	m_{T}	p_{T}^{ℓ}	m_{T}	p_{T}^{ℓ}	m_{T}
δm_W [MeV]						
$\langle\mu\rangle$ scale factor	0.2	1.0	0.2	1.0	0.2	1.0
$\Sigma\vec{E}_{\mathrm{T}}$ correction	0.9	12.2	1.1	10.2	1.0	11.2
Residual corrections (statistics)	2.0	2.7	2.0	2.7	2.0	2.7
Residual corrections (interpolation)	1.4	3.1	1.4	3.1	1.4	3.1
Residual corrections ($Z \to W$ extrapolation)	0.2	5.8	0.2	4.3	0.2	5.1
Total	2.6	14.2	2.7	11.8	2.6	13.0

Consistency tests with Z-boson events

Event selection requirements:

- W selection requirements including $p_{\mathrm{T}}^{\ell\ell} < 30$ GeV
- $p_{\mathrm{T}}^{\mathrm{miss}}$ in Z events defined by treating one of the two decay leptons as a neutrino

Background contribution:

- Top-quark and electroweak using MC samples (0.12%)
- Multijet in the muon channel using $b\bar{b}$ and $c\bar{c}$ MC samples ($< 0.05\%$, neglected)
- Multijet in the electron channel using a data-driven estimate (0.1%)

m_Z extracted with template fits to the $m_{\ell\ell}$, p_{T}^{ℓ} and m_{T} kinematic distributions:

- Templates generated with values of m_Z in steps of 4 to 25 MeV within a range of ± 450 MeV centred in the LEP value
- m_Z determined by minimising the χ^2 function of the compatibility test between the templates and the measured distributions
- The χ^2 function is interpolated with a second order polynomial
- $m_{\ell\ell}$ distribution used for the extraction in the range $[80, 100]$ GeV:
  $\Rightarrow$ closure test of the lepton calibration procedures
  $\Rightarrow \Delta m_Z = 1 \pm 3$ MeV in the muon channel and $\Delta m_Z = 3 \pm 5$ MeV in the electron channel
- p_{T}^{ℓ} distribution used for the extraction in the range $[30, 55]$ GeV:
  $\Rightarrow$ tests the physics modelling and efficiency corrections
  $\Rightarrow$ the compatibility with the reference value of m_Z at the level of 0.9σ
- m_{T} distribution used for the extraction in the range $[40, 120]$ GeV:
  $\Rightarrow$ test of the recoil calibration
  $\Rightarrow$ the compatibility with the reference value of m_Z at the level of 1.5σ

Consistency tests with Z-boson events

$p_{\mathrm{T}}^{\ell\ell}$ and $y_{\ell\ell}$ distributions, not sensitive to m_Z

⇒ Detector calibration & physics-modelling corrections applied to the simulated events

⇒ Data and simulation agree at the level of 1-2% in all the distributions

⇒ Background events contribute less than 0.2% of the observed distributions

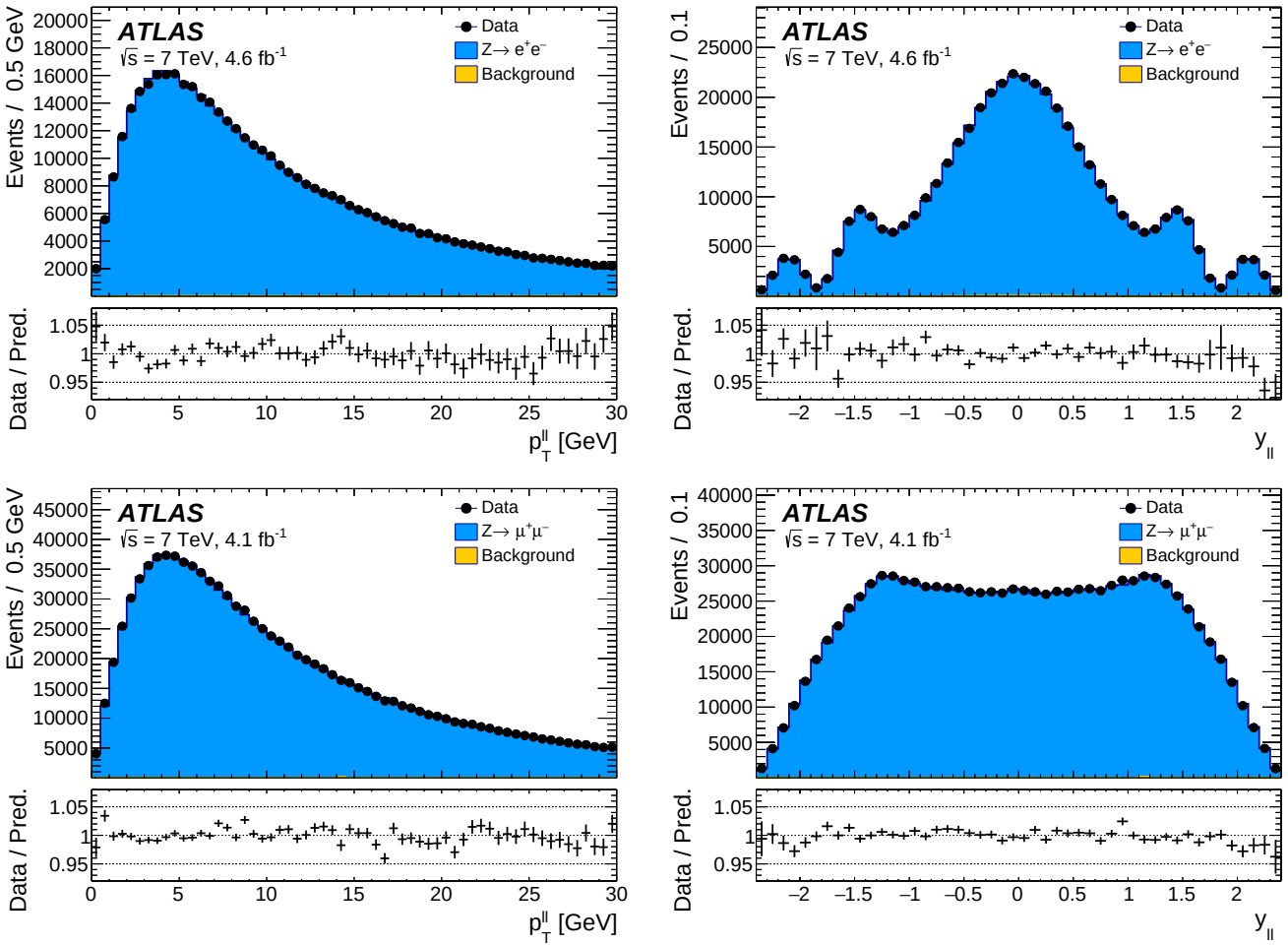

Consistency tests with Z-boson events

p_{T}^{ℓ} and m_{T} distributions, sensitive to m_Z

⇒ Detector calibration & physics-modelling corrections applied to the simulated events

⇒ Data and simulation agree at the level of 1-2% in all the distributions

⇒ Background events contribute less than 0.2% of the observed distributions

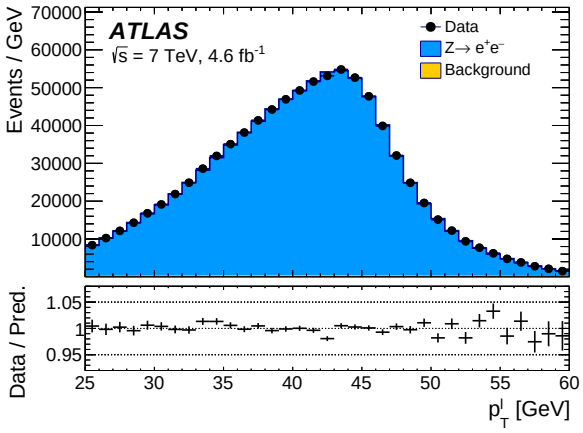

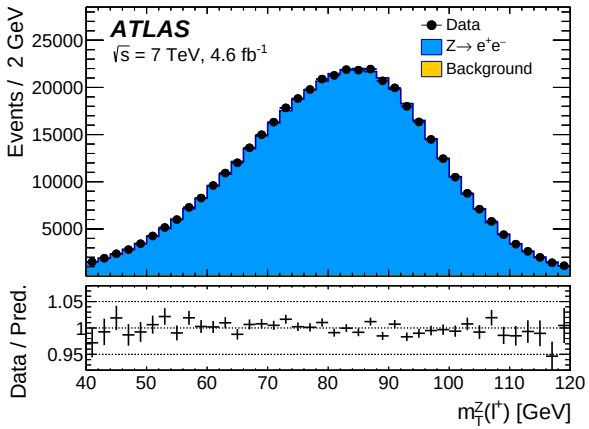

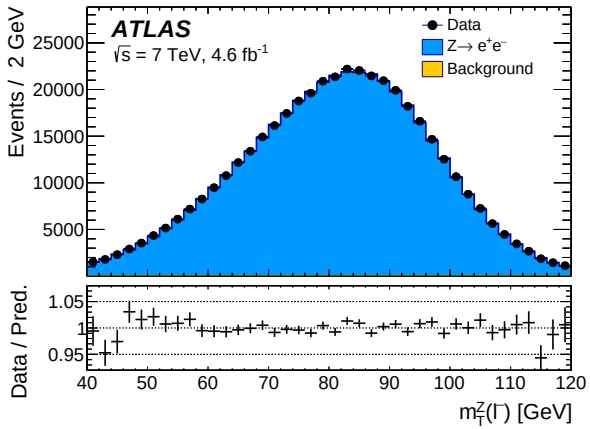

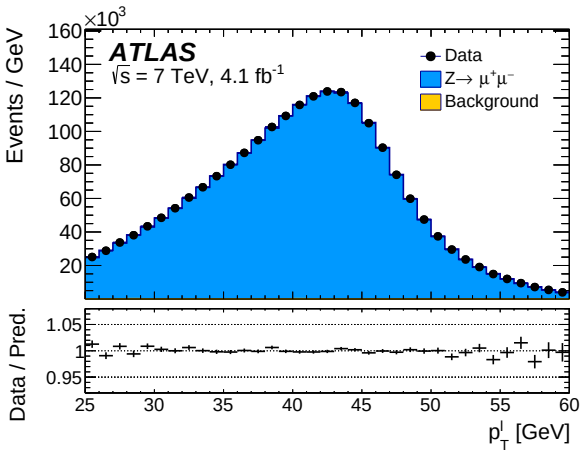

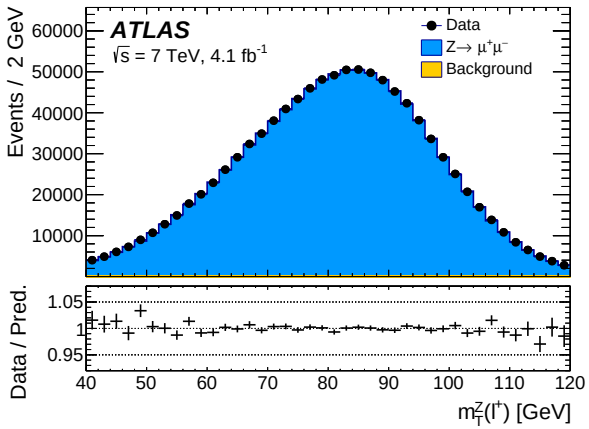

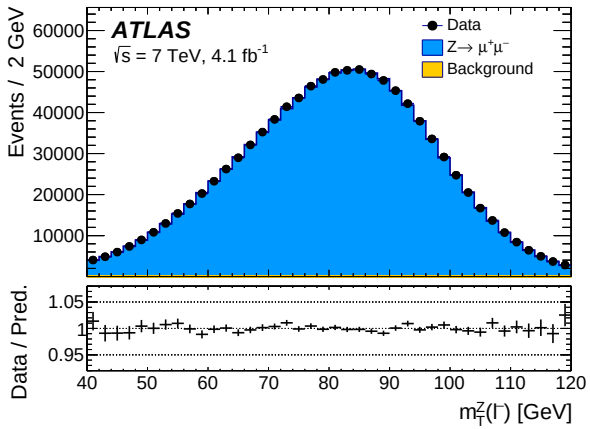

Background estimation

Background contributions:

- $Z \to \ell\ell$: POWHEG+PYTHIA 8
  (up to 4.0% in the electron channel and 6.3% in the muon channel)
- $Z \to \tau\tau$: POWHEG+PYTHIA 8 (0.12%)
- $W \to \tau\nu$: POWHEG+PYTHIA 8 (1.0%)
- Top-quark backgrounds: MC@NLO interfaced to HERWIG and JIMMY (0.11%)
- Dibosons (WW, WZ, ZZ): HERWIG (0.07%)
- Multijet background: data-driven, relies on template fits to kinematic distributions ($p_{\mathrm{T}}^{\mathrm{miss}}$, m_{T} and $p_{\mathrm{T}}^{\ell}/m_{\mathrm{T}}$) in background-dominated regions (FR1 and FR2)

Template fits are done in slices of isolation and then the final multijet fraction is extrapolated to the SR isolation

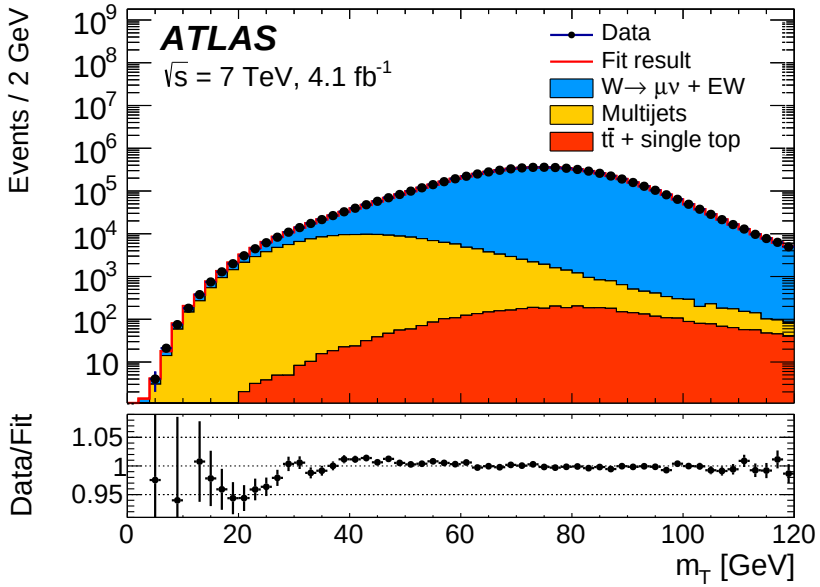

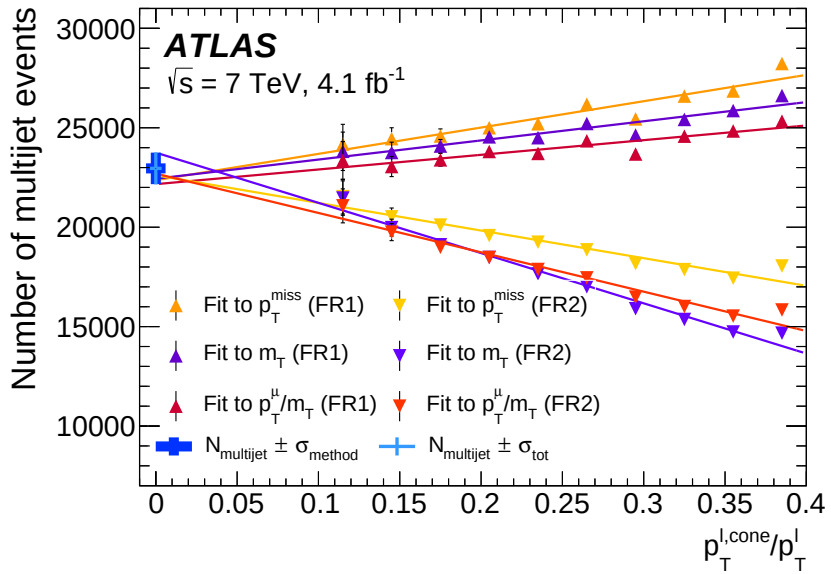

Multijet background estimation

- Multijet background contribution estimated using template fits to kinematic distributions in background-dominated regions
- Multijet background templates:
  - Obtained from data by inverting the lepton energy-isolation requirements
  - Contamination by electroweak and top production, estimated using simulation, subtracted
- Observables used for the template fits:
  - $p_{\mathrm{T}}^{\mathrm{miss}}$
  - m_{T}
  - $p_{\mathrm{T}}^{\ell}/m_{\mathrm{T}}$
- Two kinematic regions:
  - FR1 (removing $p_{\mathrm{T}}^{\mathrm{miss}}$ and m_{T} requirements)
  - FR2 (removing $p_{\mathrm{T}}^{\mathrm{miss}}$, m_{T} and u_{T} requirements)

Multijet background estimation

Template fits

- FR1 kinematic region
- Multijet templates derived from the data requiring:

  $\Rightarrow 4 < p_{\mathrm{T}}^{e,\mathrm{cone}} < 8$ GeV in the electron channel

  $\Rightarrow 0.2 < p_{\mathrm{T}}^{\mu,\mathrm{cone}}/p_{\mathrm{T}}^{\ell} < 0.4$ in the muon channel

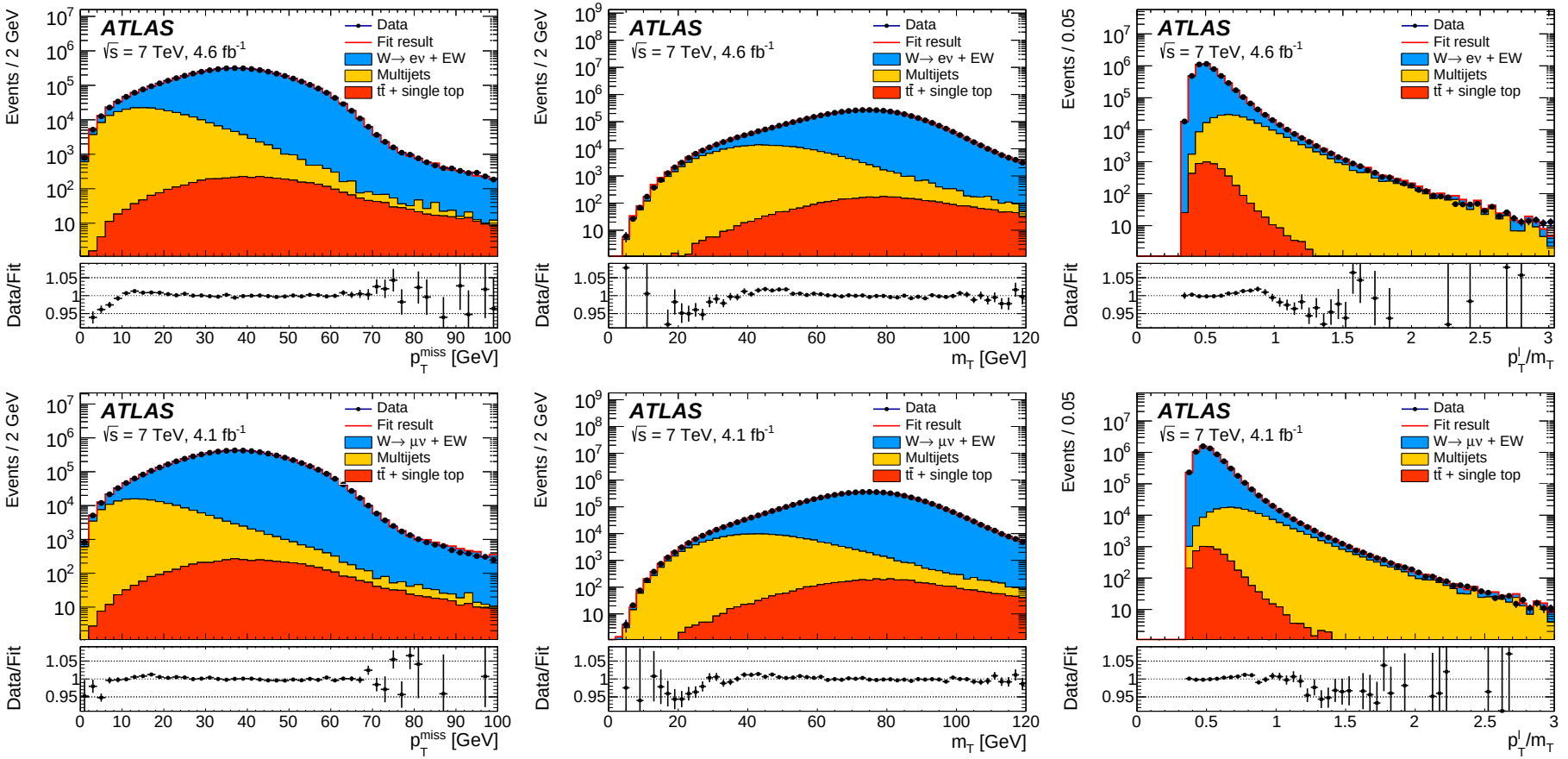

Multijet background estimation

⇒ Estimated number of multijet-background events as a function of the lower bound of the isolation- variable range used to define the control regions

⇒ Estimation performed for the two regions (FR1 and FR2) and the three distributions ($p_{\mathrm{T}}^{\mathrm{miss}}$, m_{T} and $p_{\mathrm{T}}^{\ell}/m_{\mathrm{T}}$)

Electron channel

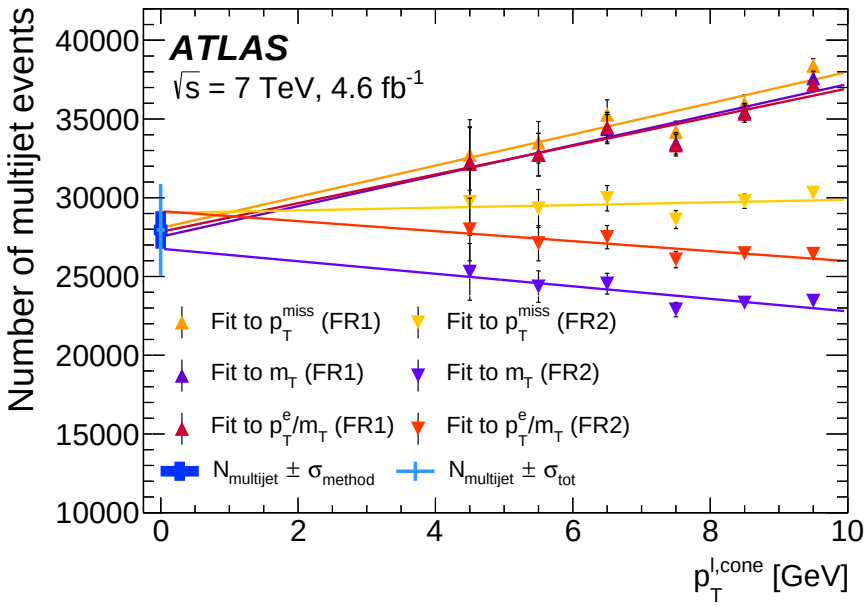

Muon channel

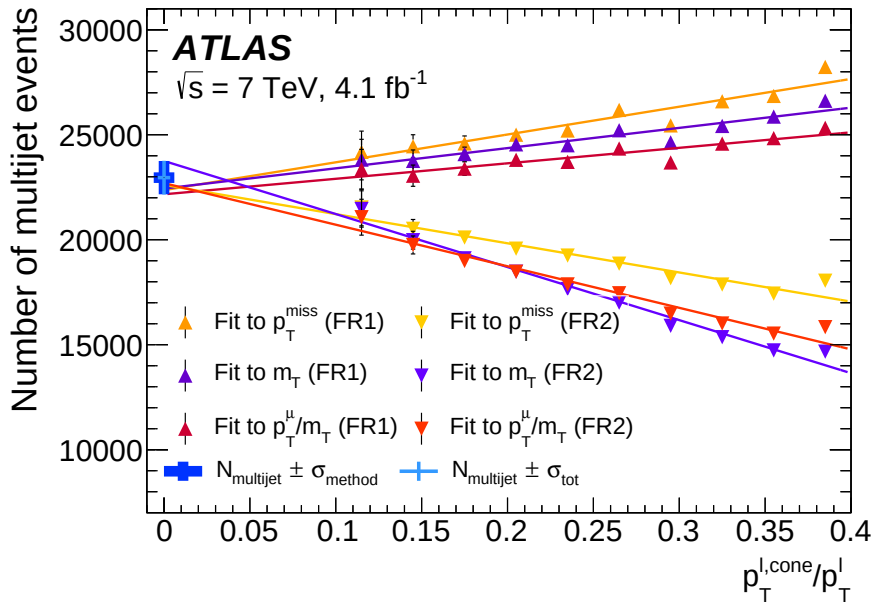

Background estimation

⇒ Impact of the background systematic uncertainties on the determination of m_W

Kinematic distribution	p_{T}^{ℓ}				m_{T}			
Decay channel	$W \to e\nu$		$W \to \mu\nu$		$W \to e\nu$		$W \to \mu\nu$	
W-boson charge	W^+	W^-	W^+	W^-	W^+	W^-	W^+	W^-
δm_W [MeV]								
$W \to \tau\nu$ (fraction, shape)	0.1	0.1	0.1	0.2	0.1	0.2	0.1	0.3
$Z \to ee$ (fraction, shape)	3.3	4.8	–	–	4.3	6.4	–	–
$Z \to \mu\mu$ (fraction, shape)	–	–	3.5	4.5	–	–	4.3	5.2
$Z \to \tau\tau$ (fraction, shape)	0.1	0.1	0.1	0.2	0.1	0.2	0.1	0.3
WW, WZ, ZZ (fraction)	0.1	0.1	0.1	0.1	0.4	0.4	0.3	0.4
Top (fraction)	0.1	0.1	0.1	0.1	0.3	0.3	0.3	0.3
Multijet (fraction)	3.2	3.6	1.8	2.4	8.1	8.6	3.7	4.6
Multijet (shape)	3.8	3.1	1.6	1.5	8.6	8.0	2.5	2.4
Total	6.0	6.8	4.3	5.3	12.6	13.4	6.2	7.4

Control distributions

η_ℓ, u_T and $u_\parallel^\ell$ distributions for W^+ and W^- events in the electron channel

$\Rightarrow$ Detector calibration and the physics modelling validated comparing data and signal and background expectations for several kinematic distributions insensitive to m_W

$\Rightarrow$ Data and simulation agree for all distributions

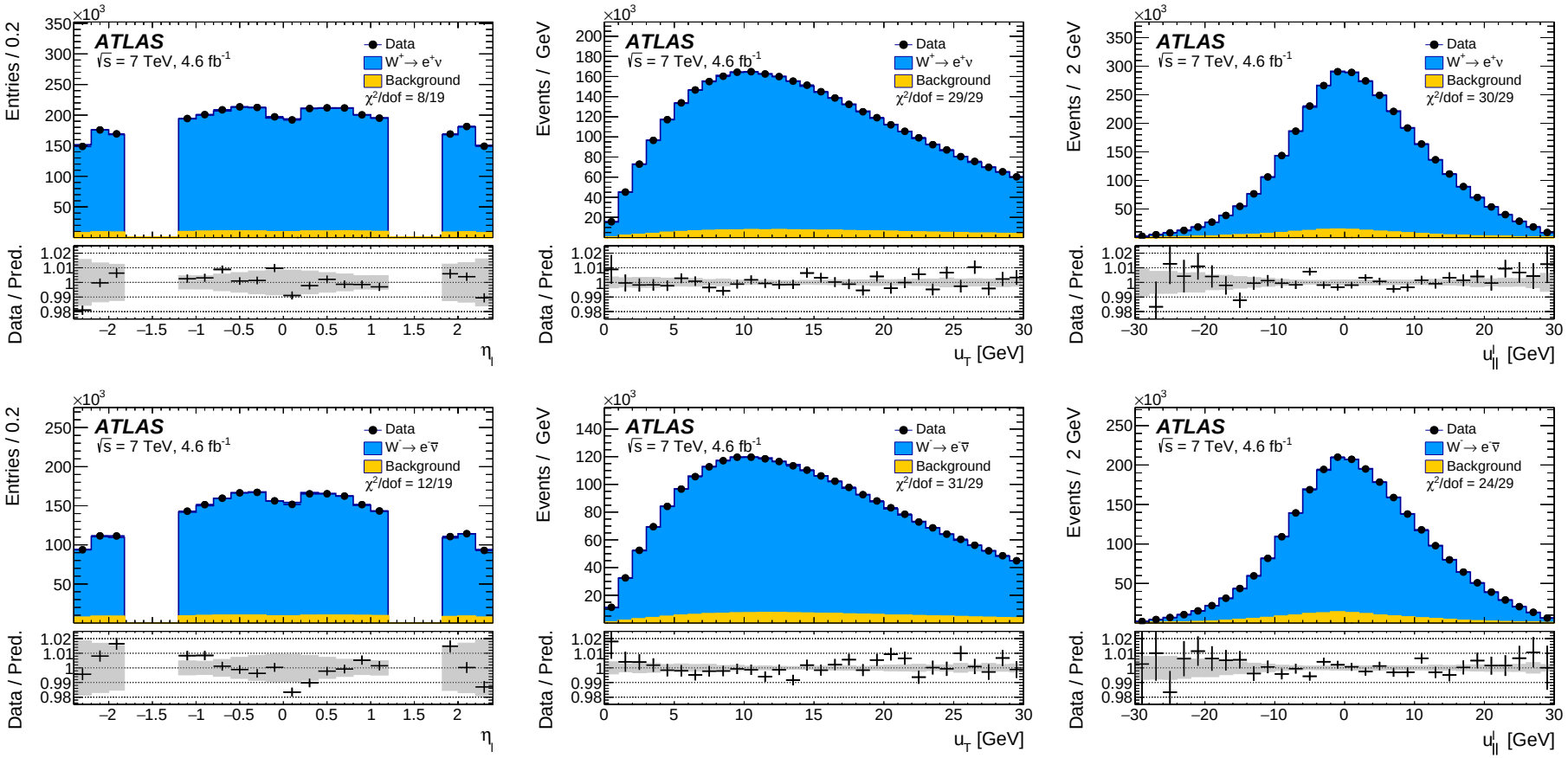

Control distributions

η_ℓ, u_T and $u_\parallel^\ell$ distributions for W^+ and W^- events in the muon channel

$\Rightarrow$ Detector calibration and the physics modelling validated comparing data and signal and background expectations for several kinematic distributions insensitive to m_W

$\Rightarrow$ Data and simulation agree for all distributions

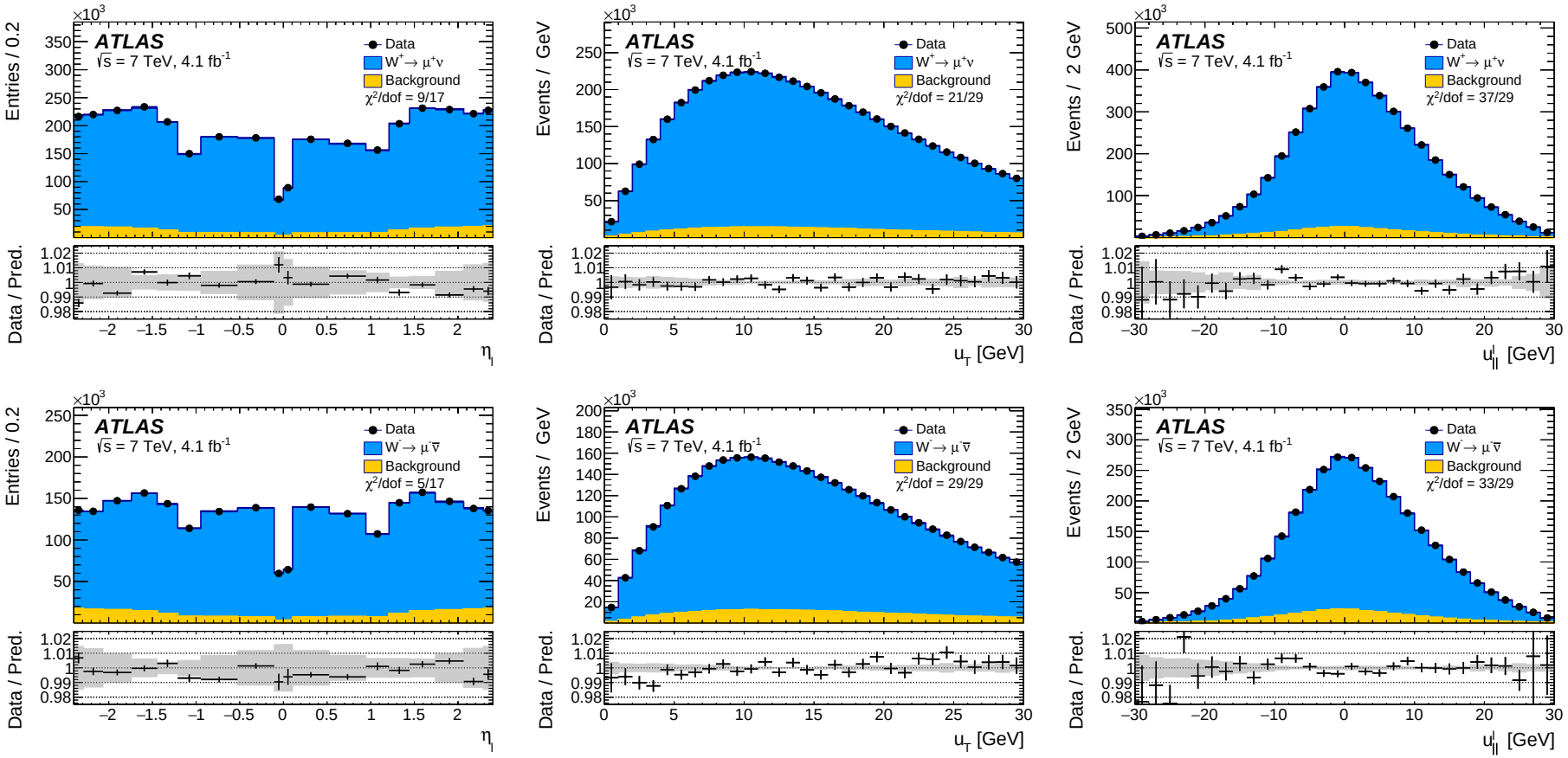

Mass-sensitive distributions

p_{T}^{ℓ} distributions for W^+ and W^- events in the electron and muon channels

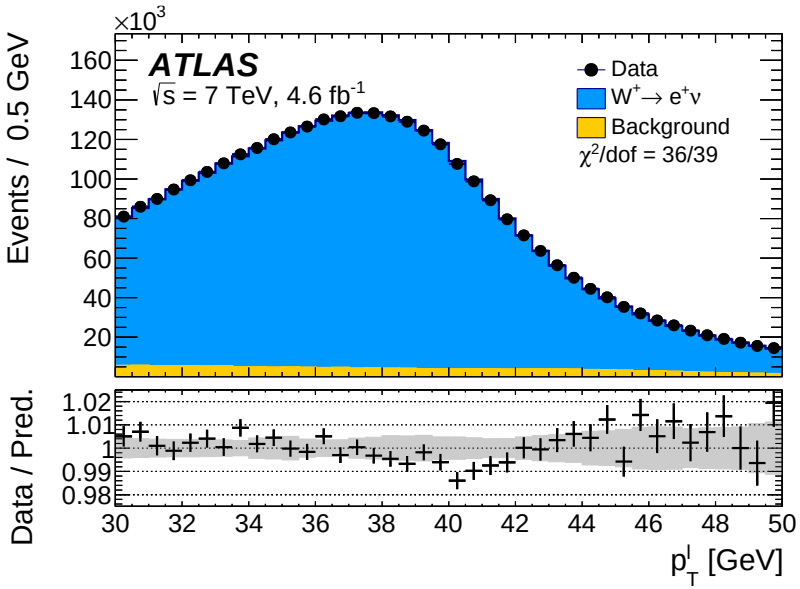

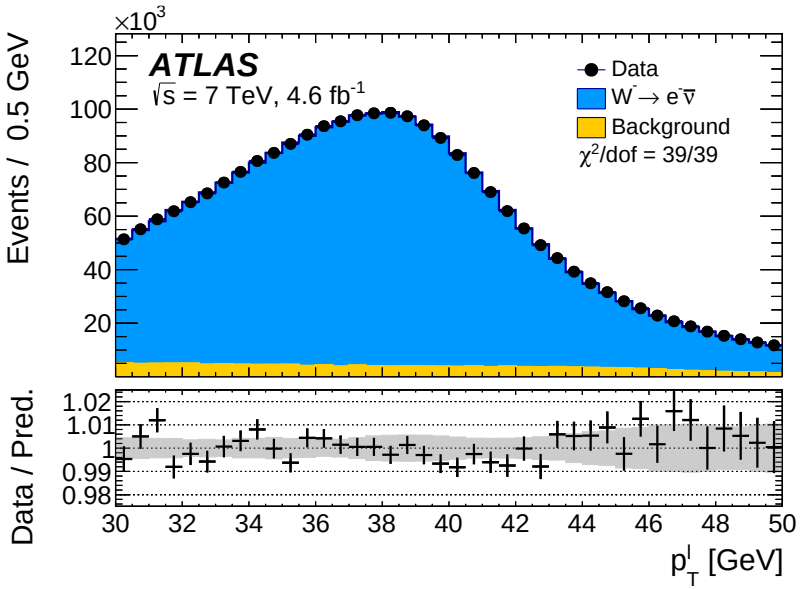

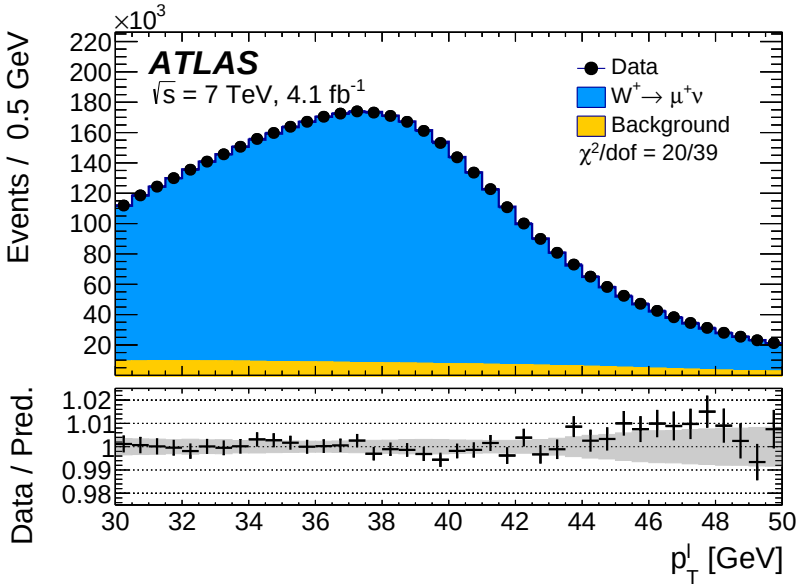

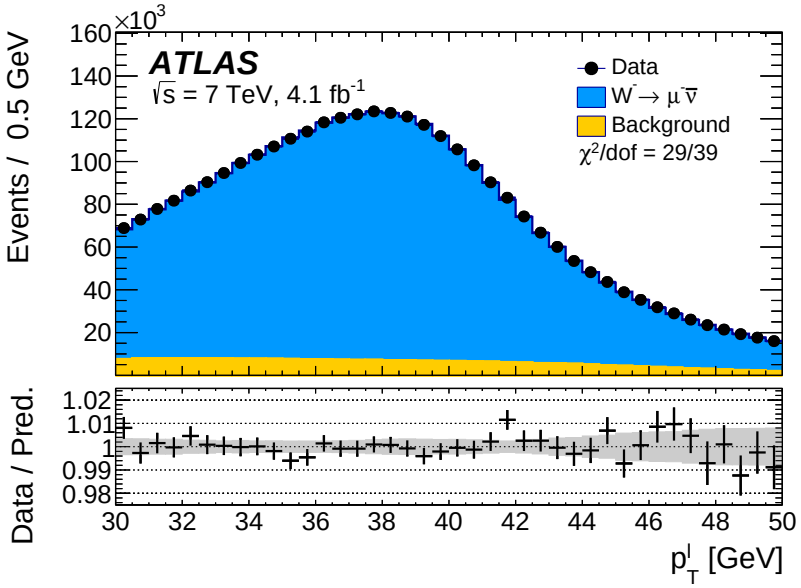

Mass-sensitive distributions

m_T distributions for W^+ and W^- events in the electron and muon channels

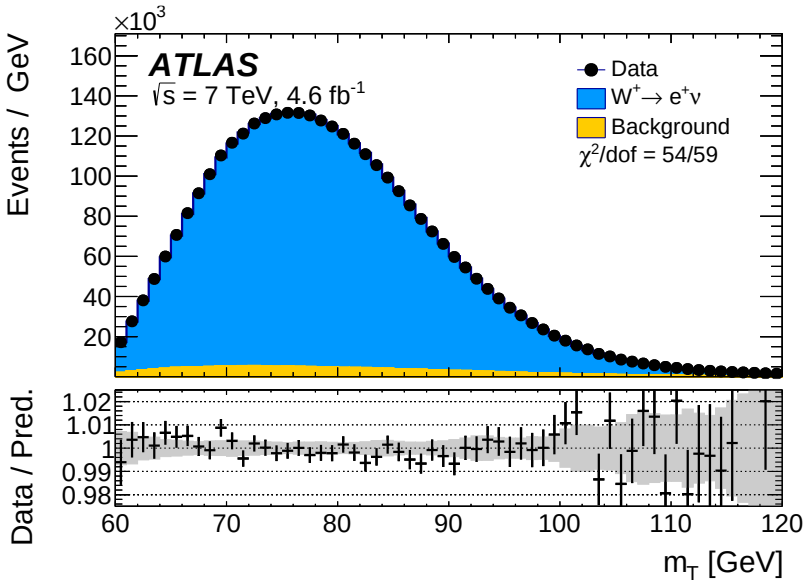

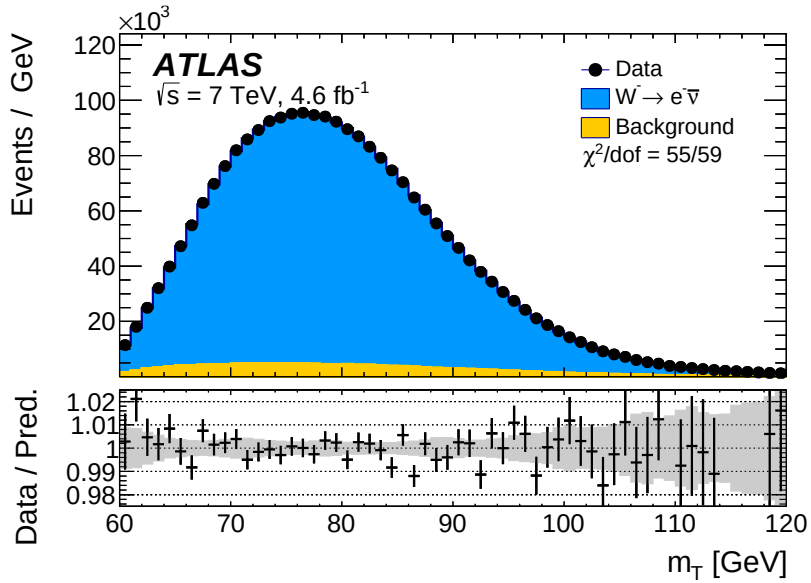

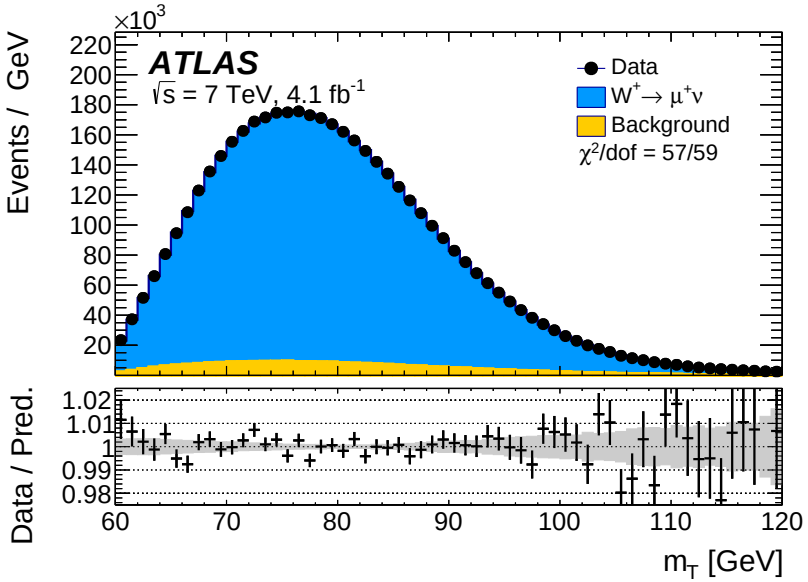

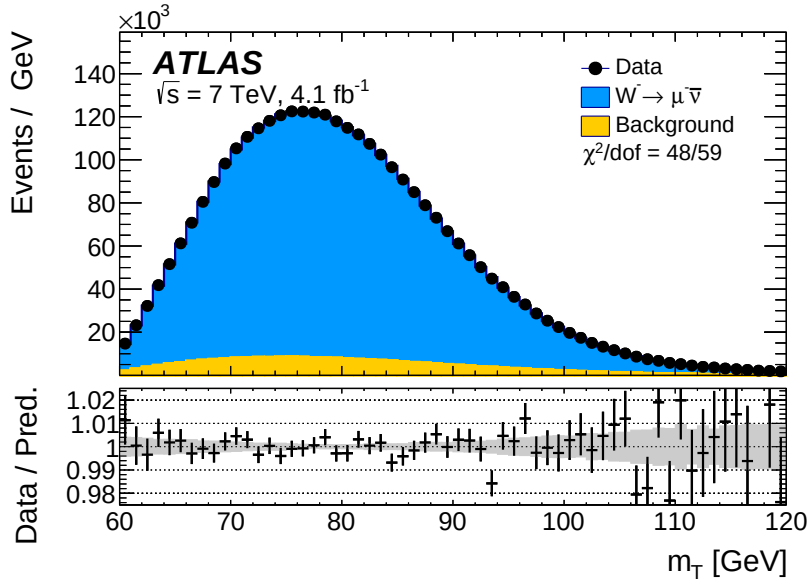

Mass-sensitive distributions

$p_{\mathrm{T}}^{\mathrm{miss}}$ distributions for W^+ and W^- events in the electron and muon channels

$\Rightarrow$ Used as cross-check

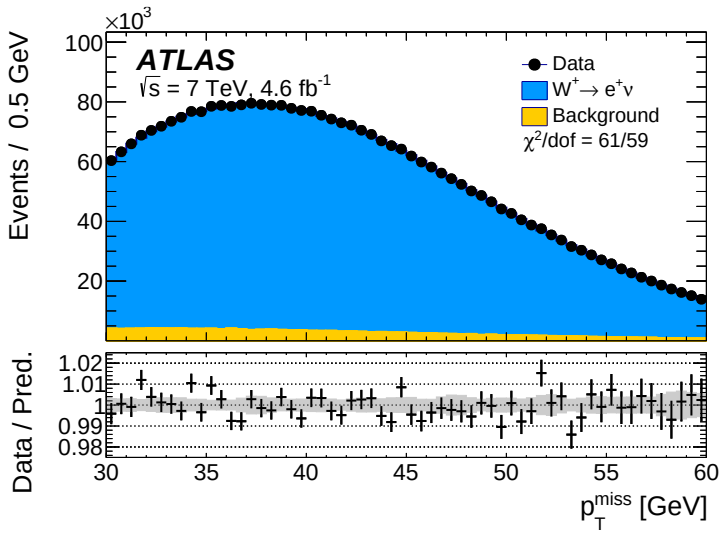

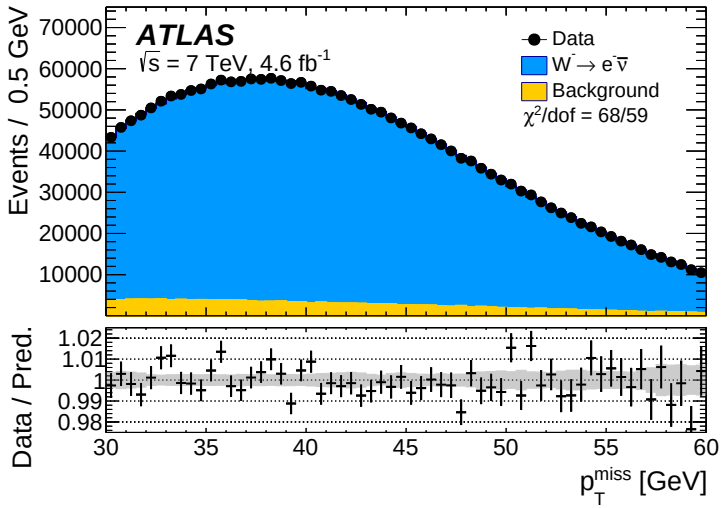

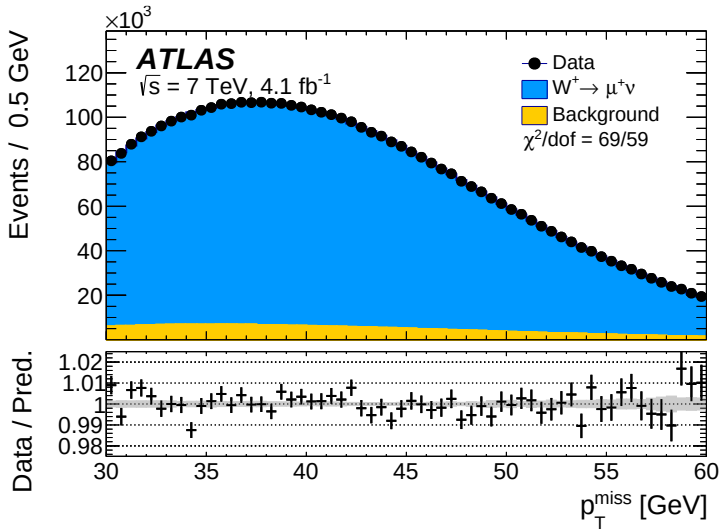

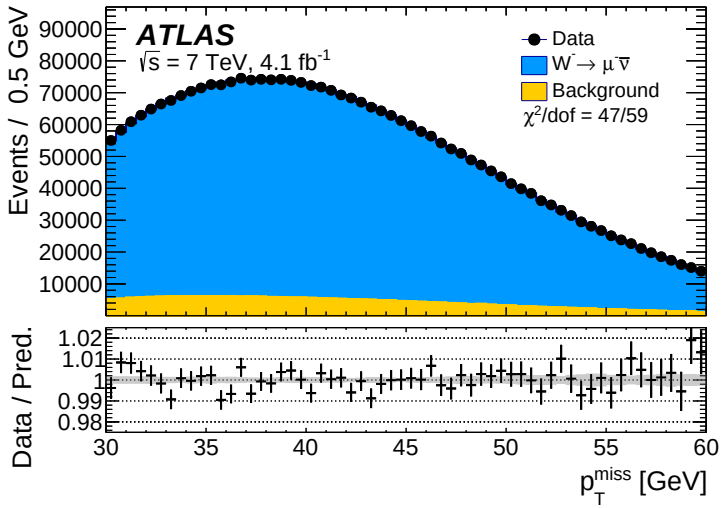

Results

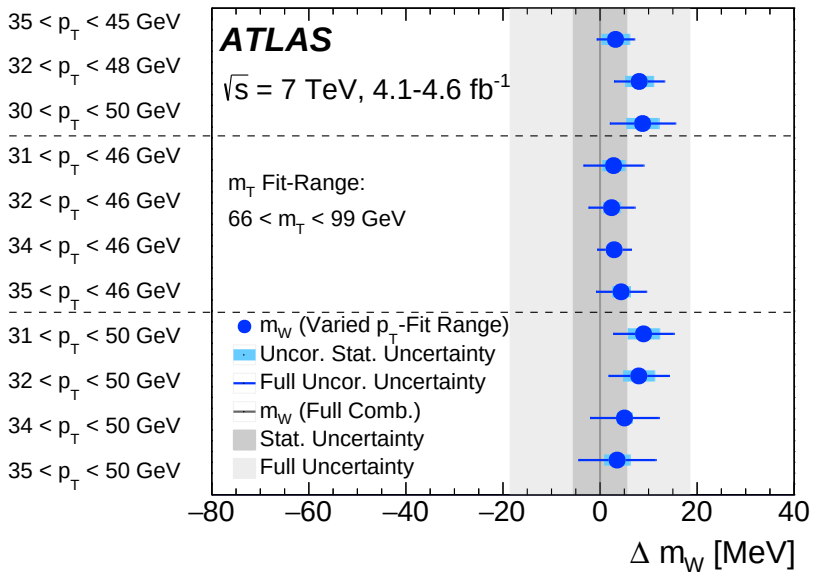
35 < p_T < 45 GeV
32 < p_T < 48 GeV
30 < p_T < 50 GeV
31 < p_T < 46 GeV
32 < p_T < 46 GeV
34 < p_T < 46 GeV
35 < p_T < 46 GeV
31 < p_T < 50 GeV
32 < p_T < 50 GeV
34 < p_T < 50 GeV
35 < p_T < 50 GeV
ATLAS
√s = 7 TeV, 4.1-4.6 fb-1
m_T Fit-Range:
66 < m_T < 99 GeV
m_W (Varied p_T-Fit Range)
Uncor. Stat. Uncertainty
Full Uncor. Uncertainty
m_W (Full Comb.)
Stat. Uncertainty
Full Uncertainty
–80 –60 –40 –20 0 20 40
Δ m_W [MeV]

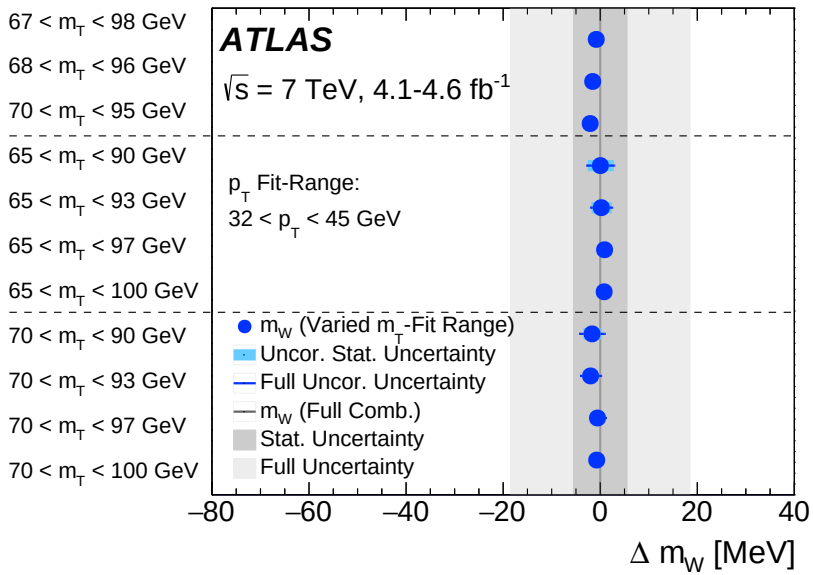
67 < m_T < 98 GeV
68 < m_T < 96 GeV
70 < m_T < 95 GeV
65 < m_T < 90 GeV
65 < m_T < 93 GeV
65 < m_T < 97 GeV
65 < m_T < 100 GeV
70 < m_T < 90 GeV
70 < m_T < 93 GeV
70 < m_T < 97 GeV
70 < m_T < 100 GeV
ATLAS
√s = 7 TeV, 4.1-4.6 fb-1
p_T Fit-Range:
32 < p_T < 45 GeV
m_W (Varied m_T-Fit Range)
Uncor. Stat. Uncertainty
Full Uncor. Uncertainty
m_W (Full Comb.)
Stat. Uncertainty
Full Uncertainty
–80 –60 –40 –20 0 20 40
Δ m_W [MeV]

Results in the different categories

Channel m_{T}-Fit	m_W [MeV]	Stat. Unc.	Muon Unc.	Elec. Unc.	Recoil Unc.	Bckg. Unc.	QCD Unc.	EW Unc.	PDF Unc.	Total Unc.
$W^+ \to \mu\nu, \lvert\eta\rvert < 0.8$	80371.3	29.2	12.4	0.0	15.2	8.1	9.9	3.4	28.4	47.1
$W^+ \to \mu\nu, 0.8 < \lvert\eta\rvert < 1.4$	80354.1	32.1	19.3	0.0	13.0	6.8	9.6	3.4	23.3	47.6
$W^+ \to \mu\nu, 1.4 < \lvert\eta\rvert < 2.0$	80426.3	30.2	35.1	0.0	14.3	7.2	9.3	3.4	27.2	56.9
$W^+ \to \mu\nu, 2.0 < \lvert\eta\rvert < 2.4$	80334.6	40.9	112.4	0.0	14.4	9.0	8.4	3.4	32.8	125.5
$W^- \to \mu\nu, \lvert\eta\rvert < 0.8$	80375.5	30.6	11.6	0.0	13.1	8.5	9.5	3.4	30.6	48.5
$W^- \to \mu\nu, 0.8 < \lvert\eta\rvert < 1.4$	80417.5	36.4	18.5	0.0	12.2	7.7	9.7	3.4	22.2	49.7
$W^- \to \mu\nu, 1.4 < \lvert\eta\rvert < 2.0$	80379.4	35.6	33.9	0.0	10.5	8.1	9.7	3.4	23.1	56.9
$W^- \to \mu\nu, 2.0 < \lvert\eta\rvert < 2.4$	80334.2	52.4	123.7	0.0	11.6	10.2	9.9	3.4	34.1	139.9
$W^+ \to e\nu, \lvert\eta\rvert < 0.6$	80352.9	29.4	0.0	19.5	13.1	15.3	9.9	3.4	28.5	50.8
$W^+ \to e\nu, 0.6 < \lvert\eta\rvert < 1.2$	80381.5	30.4	0.0	21.4	15.1	13.2	9.6	3.4	23.5	49.4
$W^+ \to e\nu, 1,8 < \lvert\eta\rvert < 2.4$	80352.4	32.4	0.0	26.6	16.4	32.8	8.4	3.4	27.3	62.6
$W^- \to e\nu, \lvert\eta\rvert < 0.6$	80415.8	31.3	0.0	16.4	11.8	15.5	9.5	3.4	31.3	52.1
$W^- \to e\nu, 0.6 < \lvert\eta\rvert < 1.2$	80297.5	33.0	0.0	18.7	11.2	12.8	9.7	3.4	23.9	49.0
$W^- \to e\nu, 1.8 < \lvert\eta\rvert < 2.4$	80423.8	42.8	0.0	33.2	12.8	35.1	9.9	3.4	28.1	72.3
p_{T}-Fit										
$W^+ \to \mu\nu, \lvert\eta\rvert < 0.8$	80327.7	22.1	12.2	0.0	2.6	5.1	9.0	6.0	24.7	37.3
$W^+ \to \mu\nu, 0.8 < \lvert\eta\rvert < 1.4$	80357.3	25.1	19.1	0.0	2.5	4.7	8.9	6.0	20.6	39.5
$W^+ \to \mu\nu, 1.4 < \lvert\eta\rvert < 2.0$	80446.9	23.9	33.1	0.0	2.5	4.9	8.2	6.0	25.2	49.3
$W^+ \to \mu\nu, 2.0 < \lvert\eta\rvert < 2.4$	80334.1	34.5	110.1	0.0	2.5	6.4	6.7	6.0	31.8	120.2
$W^- \to \mu\nu, \lvert\eta\rvert < 0.8$	80427.8	23.3	11.6	0.0	2.6	5.8	8.1	6.0	26.4	39.0
$W^- \to \mu\nu, 0.8 < \lvert\eta\rvert < 1.4$	80395.6	27.9	18.3	0.0	2.5	5.6	8.0	6.0	19.8	40.5
$W^- \to \mu\nu, 1.4 < \lvert\eta\rvert < 2.0$	80380.6	28.1	35.2	0.0	2.6	5.6	8.0	6.0	20.6	50.9
$W^- \to \mu\nu, 2.0 < \lvert\eta\rvert < 2.4$	80315.2	45.5	116.1	0.0	2.6	7.6	8.3	6.0	32.7	129.6
$W^+ \to e\nu, \lvert\eta\rvert < 0.6$	80336.5	22.2	0.0	20.1	2.5	6.4	9.0	5.3	24.5	40.7
$W^+ \to e\nu, 0.6 < \lvert\eta\rvert < 1.2$	80345.8	22.8	0.0	21.4	2.6	6.7	8.9	5.3	20.5	39.4
$W^+ \to e\nu, 1,8 < \lvert\eta\rvert < 2.4$	80344.7	24.0	0.0	30.8	2.6	11.9	6.7	5.3	24.1	48.2
$W^- \to e\nu, \lvert\eta\rvert < 0.6$	80351.0	23.1	0.0	19.8	2.6	7.2	8.1	5.3	26.6	42.2
$W^- \to e\nu, 0.6 < \lvert\eta\rvert < 1.2$	80309.8	24.9	0.0	19.7	2.7	7.3	8.0	5.3	20.9	39.9
$W^- \to e\nu, 1.8 < \lvert\eta\rvert < 2.4$	80413.4	30.1	0.0	30.7	2.7	11.5	8.3	5.3	22.7	51.0